# Heavy quark diffusion in a Polyakov loop plasma

Balbeer Singh,[1,2] Aman Abhishek,[1,2] Santosh K. Das,[3] and Hiranmaya Mishra[1]

[1]*Theory Division, Physical Research Laboratory, Navrangpura, Ahmedabad 380 009, India*
[2]*Indian Institute of Technology Gandhinagar, Gandhinagar 382 355, Gujarat, India*
[3]*School of Physical Sciences, Indian Institute of Technology Goa, Ponda-403401, Goa, India*

(Received 10 January 2019; revised manuscript received 30 May 2019; published 11 December 2019)

We calculate the transport coefficients, drag, and momentum diffusion of a heavy quark in a thermalized plasma of light quarks in the background of a Polyakov loop. The quark thermal mass and the gluon Debye mass are calculated in a nontrivial Polyakov loop background. The constituent quark masses and the Polyakov loop are estimated within a Polyakov loop quark-meson (PQM) model. The relevant scattering amplitudes for heavy quarks and light partons in the background of a Polyakov loop have been estimated within the matrix model. We have also compared the results with the Polyakov loop parameter estimated from lattice QCD simulations. We have studied the temperature and momentum dependence of heavy quark drag and diffusion coefficients. It is observed that the temperature dependence of the drag coefficient is quite weak, which may play a key role in understanding heavy quark observables at Relativistic Heavy Ion Collider and Large Hadron Collider energies.

DOI: 10.1103/PhysRevD.100.114019

## I. INTRODUCTION

Experimental heavy ion collision (HIC) programs at the Relativistic Heavy Ion Collider (RHIC) and at the Large Hadron Collider (LHC) indicate the production of a liquidlike phase of matter, having a remarkably small ratio of shear viscosity to entropy density, $\eta/s \approx 0.1$, where the properties of the system are governed by quarks and gluons. Such a state of matter is known as quark-gluon plasma (QGP) [1,2]. To characterize the properties of QGP, penetrating and well-calibrated probes are essential. In this context, the heavy quarks (HQs) [3–9], mainly charm and bottom, play a crucial role, since they do not constitute the bulk part of the matter owing to their larger mass compared to the temperature created in heavy ion collisions. Also, thermal production of heavy quarks is negligible, due to their large masses, in the QGP within the range of temperatures that can be achieved at RHIC and LHC colliding energies.

Heavy quarks are exclusively created in hard processes which can be handled by perturbative QCD calculations [10], and therefore their initial distribution is theoretically known and can be verified by experiment. They interact with the plasma constituents, the light quarks, and the gluons, but their initial spectrum is too hard to come to equilibrium with the medium. Therefore, the high-momentum heavy quark spectrum carries the information of their interaction with the plasma particles during the expansion of the hot and dense fireball and on the plasma properties. Since the light quark, antiquark, and gluons are thermalized, the heavy quark interaction with the light constituents leads to a Brownian motion which can be treated with the framework of a Fokker-Planck equation. Thus, the interaction of the heavy quark in QGP is contained in the drag and diffusion coefficients of the heavy quark. The resulting momentum distribution of the heavy mesons, which depends upon the drag and diffusion coefficients, gets reflected in the nuclear modification factor ($R_{AA}$), which is measured experimentally.

Initially, pQCD predicted a small nuclear suppression factor [11,12], $R_{AA}$, in nucleus-nucleus collisions in comparison with the proton-proton collisions. The first experimental data [13–15] on heavy quarks suggest a strong nuclear suppression factor which cannot be explained within the pQCD framework. Several attempts [16–33] have been made by different groups to study the heavy quark interaction in QGP, going beyond pQCD to include the nonperturbative effects. Quasiparticle models enjoy considerable success in describing heavy quark dynamics in QGP [20,24].

In the present study, we are making a first attempt to study heavy quark transport coefficients in QGP including the nonperturbative effects through a background gauge field (the Polyakov loop background) and chiral condensate. The Polyakov loop manifests itself in the transport coefficient in two ways. First, it is seen through the Debye mass that enters when calculating the scattering of the heavy quark off of light thermal partons. It also enters nontrivially in the statistical distribution of the light partons in a nonperturbative medium. Indeed, both of the effects arising from the Polyakov loop and quark condensate are important near the transition temperature. The value of the normalized Polyakov loop is about half its asymptotic value at the critical temperature in different low-energy effective models like Polyakov Nambu–Jona-Lasinio (PNJL) models [34–36] or Polyakov quark-meson (PQM) [37–42] models. Similarly, the chiral condensate remains significantly finite at temperatures around the critical temperature. Effects of the Polyakov loop have been studied in various contexts such as dilepton and photon production [43] and heavy quark energy loss [44]. Significant effects have been found by including these nonperturbative features. To estimate the quark masses and the Debye mass, we therefore need the value of the Polyakov loop as a function of temperature. We do so in two different approaches. One is phenomenological in the sense that we take the Polyakov loop value as a function of temperature from the PQM model. The other approach is to take the same from lattice QCD simulations.

This paper is organized as follows: In Sec. II, we give the formalism for calculating the drag and diffusion of heavy quarks by employing the Boltzmann equation in soft momentum exchange between heavy quarks and the bulk medium [45]. In Sec. III, we recapitulate and summarize the calculation of the Debye mass and the quark thermal mass in a Polyakov loop background, as has been outlined in Refs. [43,46]. In these calculations, we have also kept the effects of a possible finite quark mass. Such an effect can be important near the transition temperature, where the light quark condensates could still be relevant. The drag and the diffusion coefficients are evaluated in Sec. IV, where we discuss their behavior as a function of temperature as well as momentum. Finally, in Sec. V, we summarize the results and present a possible outlook. We summarize the salient features of the PQM model in Appendix A. Further, in Appendix B, we give some details of the calculation for the square of matrix elements for the relevant $2 \rightarrow 2$ processes.

## II. FORMALISM

In the QGP phase, the Boltzmann equation for the charm quark distribution function, neglecting any mean-field term, can be written as [45,47]

$$\frac{\partial f_{HQ}}{\partial t} = \left[\frac{\partial f_{HQ}}{\partial t}\right]_{\mathrm{col}}, \tag{1}$$

where $f_{HQ}$ represents the spatially integrated nonequilibrium distribution function for the heavy quark. The right-hand side of Eq. (1) is the collision integral, where the phase-space distribution function of the bulk medium appears as an integrated quantity. If we define $\omega(\mathbf{p},\mathbf{k})$ as the transition rate of collisions of the heavy quark with the heat bath particles (light quarks/antiquarks and gluons) that change the heavy quark momentum from $\mathbf{p}$ to $\mathbf{p}-\mathbf{k}$, then we can write [45]

$$\left[\frac{\partial f_{HQ}}{\partial t}\right]_{\mathrm{col}} = \int d^3k[\omega(\mathbf{p}+\mathbf{k},\mathbf{k})f_{HQ}(\mathbf{p}+\mathbf{k}) - \omega(\mathbf{p},\mathbf{k})f_{HQ}(\mathbf{p})]. \tag{2}$$

The first term in the integrand represents a gain of probability through collisions which knock the charm quark into the volume element of momentum space at $\mathbf{p}$, and the second term represents the loss out of that volume element. $\omega(\mathbf{p},\mathbf{k})$ is the total contribution coming from heavy quark scattering from gluons and light quarks/antiquarks. Furthermore, assuming the scattering processes to be dominated by small momentum transfer, we can expand $\omega(\mathbf{p}+\mathbf{k},\mathbf{k})f_{HQ}(\mathbf{p}+\mathbf{k})$ around $\mathbf{k}$:

$$\begin{aligned}&\omega(\mathbf{p}+\mathbf{k},\mathbf{k})f_{HQ}(\mathbf{p}+\mathbf{k})\\ &\approx \omega(\mathbf{p},\mathbf{k})f_{HQ}(\mathbf{p}) + \mathbf{k}\cdot\frac{\partial}{\partial\mathbf{p}}(\omega f_{HQ}(\mathbf{p}))\\ &+\frac{1}{2}k_ik_j\frac{\partial^2}{\partial p_i\partial p_j}(\omega f_{HQ}(\mathbf{p})).\end{aligned} \tag{3}$$

The higher powers of the momentum transfer, $k_i$'s, are assumed to be small [48]. Keeping up to the second term and substituting in Eq. (2), we get

$$\left[\frac{\partial f_{HQ}}{\partial t}\right]_{\mathrm{col}} = \frac{\partial}{\partial p_i}\left[A_i(\mathbf{p})f_{HQ} + \frac{\partial}{\partial p_j}[B_{ij}(p)f_{HQ}]\right]. \tag{4}$$

Now Eq. (1) is reduced to the Fokker-Planck equation, where the kernels

$$\begin{aligned}A_i &= \int d\mathbf{k}\,\omega(\mathbf{p},\mathbf{k})k_i,\\ B_{ij} &= \int d\mathbf{k}\,\omega(\mathbf{p},\mathbf{k})k_ik_j\end{aligned} \tag{5}$$

stand for the drag and the diffusion coefficients, respectively. The function $\omega(\mathbf{p},\mathbf{k})$ is given by

$$\omega(\mathbf{p},\mathbf{k}) = g_{q,g}\int\frac{d\mathbf{q}}{(2\pi)^3}f_l(\mathbf{q})v\sigma_{\mathbf{p},\mathbf{q}\to\mathbf{p}-\mathbf{k},\mathbf{q}+\mathbf{k}}, \tag{6}$$

where $f_l(\mathbf{q})$ is the thermal phase-space distribution of the particles which constitute the heat bath, which in the present case stands for light quarks/antiquarks and gluons; $v = |v_p - v_q|$ is the relative velocity between the two collision partners; $\sigma$ denotes the interaction cross section; and $g_{q/g}$ is the statistical degeneracy factor for light quarks/antiquarks and gluons.

In particular, $A_i$ and $B_{ij}$, for the (generic) process $HQ(p) + l(q) \to HQ(p') + l(q')$ (where $l$ stands for light quarks and gluons), are given by [45,49–51]

$$A_i = \frac{1}{2E_p}\int \frac{d\mathbf{q}}{(2\pi)^3 E_q}\int \frac{d\mathbf{p}'}{(2\pi)^3 E'_p}\int \frac{d\mathbf{q}'}{(2\pi)^3 E'_q} \times \frac{1}{g_{HQ}}\sum |M|^2 (2\pi)^4 \delta^4(p+q-p'-q') f_l(q) \times (1\pm f_l(q'))[(p-p')_i] \equiv \langle\langle (p-p')\rangle\rangle, \tag{7}$$

where $g_{HQ}$ is the statistical degeneracy of the charm quark. The factor $f_l(q)$ denotes the thermal phase-space factor for the gluons and light quarks/antiquarks in the incident channel, and $1\pm f_l(q')$ is the final-state Bose/Fermi enhanced/suppression phase-space factor. The above expression indicates that the drag coefficient is a measure of the thermal average of the momentum transfer, $p - p'$, weighted by the elastic heavy quark bulk interaction through the square of the invariant amplitude, $|M|^2$.

Similarly, heavy quark diffusion coefficients can be defined as

$$B_{ij} = \frac{1}{2E_p}\int \frac{d\mathbf{q}}{(2\pi)^3 E_q}\int \frac{d\mathbf{p}'}{(2\pi)^3 E'_p}\int \frac{d\mathbf{q}'}{(2\pi)^3 E'_q} \times \frac{1}{g_{HQ}}\sum |M|^2 (2\pi)^4 \delta^4(p+q-p'-q') f_l(q) \times (1\pm f_l(q'))\left[\frac{1}{2}(p-p')_i (p-p')_j\right] \equiv \langle\langle (p-p')_i (p-p')_j\rangle\rangle. \tag{8}$$

From the above expression, it is clear that the diffusion coefficient is a measure of the thermal average of the square of momentum transfer weighted by the elastic heavy quark bulk interaction through the square of the invariant amplitude, $|M|^2$. Since $A_i$ and $B_{ij}$ depend only on the vector $\mathbf{p}$, we may write [45]

$$A_i = p_i A, \tag{9}$$

$$B_{ij} = \left(\delta_{ij} - \frac{p_i p_j}{\mathbf{p}^2}\right) B_0 + \frac{p_i p_j}{\mathbf{p}^2} B_1, \tag{10}$$

where

$$A = p_i A_i / \mathbf{p}^2 = \langle\langle 1\rangle\rangle - \frac{\langle\langle \mathbf{p}.\mathbf{p}'\rangle\rangle}{\mathbf{p}^2}, \tag{11}$$

$$B_0 = \frac{1}{2}\left(\delta_{ij} - \frac{p_i p_j}{2p^2}\right) B_{ij} = \frac{1}{4}\left[\langle\langle \mathbf{p}'^2\rangle\rangle - \frac{\langle\langle (\mathbf{p}.\mathbf{p}')^2\rangle\rangle}{\mathbf{p}^2}\right], \tag{12}$$

$$B_1 = \frac{p_i p_j}{\mathbf{p}^2} B_{ij} = \frac{1}{2}\left[\frac{\langle\langle (\mathbf{p}.\mathbf{p}')^2\rangle\rangle}{\mathbf{p}^2} - 2\langle\langle \mathbf{p}.\mathbf{p}'\rangle\rangle + \mathbf{p}^2 \langle\langle 1\rangle\rangle\right]. \tag{13}$$

The integrals appearing in the above equations can be further simplified by solving the kinematics in the center-of-mass frame of the colliding particles, and both the drag and diffusion coefficients can be defined from a single expression:

$$\langle\langle \Gamma(p')\rangle\rangle = \frac{1}{512\pi^4}\frac{1}{E_p}\int_0^\infty \int_{-1}^{1} d(\cos\theta_{cm}) \times \int_0^{2\pi} d\phi_{cm} \frac{q^2 dq d(\cos\chi)}{E_q} f(q)(1\pm f(q')) \times \frac{\lambda^{\frac{1}{2}}(s, m_C^2, m_q^2)}{\sqrt{s}} \frac{1}{g_{HQ}} \sum |M|^2 \Gamma(p'), \tag{14}$$

with an appropriate choice of $\Gamma(p')$. As in Ref. [45], we shall consider $2\to 2$ processes, which involve Coulomb scattering, i.e., $qQ\to qQ$, through gluon exchange and Compton scattering of gluons and heavy quarks, i.e., $gQ \to gQ$. In the present work, we shall estimate the scattering amplitudes in the background of a Polyakov loop. This makes the square of the corresponding matrix element as well as the distribution function dependent on the color indices [see, e.g., Eqs. (19) and (20)]. Therefore, the expression for $\langle\langle \Gamma(p')\rangle\rangle$ becomes

$$\langle\langle \Gamma(p')\rangle\rangle = \frac{1}{512\pi^4}\frac{1}{E_p}\int_0^\infty \int_{-1}^{1} d(\cos\theta_{cm}) \times \int_0^{2\pi} d\phi_{cm} \frac{q^2 dq d(\cos\chi)}{E_q} \frac{\lambda^{\frac{1}{2}}(s, m_C^2, m_q^2)}{\sqrt{s}} \frac{1}{g_{HQ}} \times \left(\sum_{abef} f(q)_e (1 - f(q')_f) |M_C|^2_{abef} + \sum_{abefgh} f(q)_{ef}(1 + f(q')_{gh}) |M_{Cm}|^2_{abefgh}\right)\Gamma(p'), \tag{15}$$

where $|M_C|^2_{abef}$ is the matrix element squared for $q^a Q^b \to q^e Q^f$, with $ab$ $(ef)$ as the initial (final) quark color indices; and $|M_{Cm}|^2{}_{abefgh}$ is the matrix element squared for $g^{ef} Q^b \to g^{gh} Q^a$ scatterings, with $ef, a$ $(gh, b)$ as the initial (final) gluon and quark color indices. Here the color indices $a, b, e, f, g, h = 1, 2, 3$ are in the fundamental representation. Furthermore, in Eq. (15), $\lambda(x, y, z) = x^2 + y^2 + z^2 - 2xy - 2yz - 2zx$ is the triangular function. $E_p$ and $m_C$ are the heavy quark energy and mass, respectively. $E_q$ is the energy of the light quark/gluon. $s$ is the Mandelstam variable. To compute the heavy quark transport coefficient, one needs, therefore, the heavy quark–light quark/gluon scattering matrix along with the thermal distribution functions, the masses of light quarks and gluons, and the Debye screening mass. The divergence in the $t$-channel diagram here is regulated by a Debye mass [45].

In the literature, several attempts have been made over the years to compute the heavy quark drag and diffusion coefficients in QGP within different models. A recent study indicates that nonperturbative contributions are essential for the simultaneous description of heavy quarks $R_{AA}$ and $v_2$ [20]. The quasiparticle model is a way to take into account the nonperturbative effect. This can be done in a number of possible ways, which differ in how the effects of QCD interactions are modeled. To study the heavy quark transport properties in QGP, the quasiparticle approaches [20,24] that have been recently used in the literature include the interaction in the effective masses of the light quark and gluons. In these quasiparticle models, the strong coupling constant [52], $g(T)$, is the only free parameter which can be obtained by making a fit of the energy density obtained by lattice QCD calculations. The main feature of the quasiparticle approach is that the resulting coupling is significantly stronger than the one obtained from the pQCD running coupling, particularly near the quark-hadron transition temperature ($T_c$). In this present study, we adopted a different model to include the nonperturbative effects. The statistical distribution function, thermal mass, and Debye mass have been obtained in the presence of a nontrivial Polyakov loop background. In the following section, we attempt to estimate the quark thermal mass and the Debye mass in a Polyakov loop background.

## III. THERMAL AND DEBYE MASSES IN A POLYAKOV LOOP BACKGROUND

In this section, we shall estimate the nonperturbative Debye screening mass and quark thermal mass in a nontrivial Polyakov loop background to be used in the estimation of the drag and diffusion coefficients using Eqs. (11) and (12). Such a calculation has been performed in detail in Refs. [43,44,46,53] using a matrix model for semi-QGP, and it has been used for estimating the ratio of shear viscosity to entropy, as well as to dilepton and photon production, and to the energy loss of heavy quarks in the medium. We recapitulate the salient features of such a calculation, including also the possible effects from a finite mass of the light quarks which can arise from a nonvanishing scalar quark/antiquark condensate.

The Polyakov loop is a particular case of the Wilson loop where the gluon field is timelike. The background gauge field can be taken as a constant diagonal matrix $A_\mu^{ab} = \delta_{\mu 0}\delta^{ab} Q^a/g$, where the color index $a$ is not summed and $g$ is the gauge field coupling constant. The Wilson line in the temporal direction is given by

$$P = \mathcal{P}\exp\left(ig\int_0^\beta d\tau A_0(x_0,\mathbf{x})\right), \tag{16}$$

where $\mathcal{P}$ denotes path ordering in imaginary time, with $\tau$ being the imaginary time $\tau{:}\,0 \to \beta$. In the mean-field level, neglecting the fluctuations, and with the choice of the time-independent constant background field, the path ordering becomes irrelevant, and one can perform the integration over imaginary time, leading to $P = \exp(ig\beta A_0)$. The trace of the Wilson line is the Polyakov loop $\phi$, given as

$$\phi(Q) = \frac{1}{3}\sum_{a=1}^{3}\exp(i\beta Q^a). \tag{17}$$

In a $SU(N)$ gauge group, the vector potential $A_0$ is traceless, so the sum over all the $Q$'s vanishes i.e., $\sum_a Q^a = 0$; for $SU(3)$, one can parametrize $Q^a = 2\pi T(-q,0,q)$, where we have introduced a dimensionless Polyakov-loop-dependent parameter "$q$" [44], so that

$$\phi = \frac{1}{3}(1 + 2\cos 2\pi q). \tag{18}$$

Physically, such a nontrivial background field $A_0$ can be thought of as an imaginary chemical potential [54]. The thermal distribution functions for the quarks/antiquarks and the gluons are given, respectively, by [43]

$$f_a(E) = \frac{1}{e^{\beta(E-iQ^a)}+1}, \quad \tilde{f}_a(E) = \frac{1}{e^{\beta(E+iQ^a)}+1}, \tag{19}$$

$$f_{ab}(E) = \frac{1}{e^{\beta(E-i(Q^a-Q^b))}-1}. \tag{20}$$

Let us note that the quark distribution function involves only one color index because these are represented in fundamental representation. For gluons, the adjoint representation leads to two fundamental indices. For three colors, the color-averaged statistical distribution function of the gluons becomes

$$\begin{aligned} f_g(E) &= \frac{1}{3^2}\sum_{a,b=1}^{3} f_{ab}(E) \\ &= \frac{1}{9}\left(\frac{3}{e^{\beta E}-1} + \frac{e^{\beta E}(6\phi-2)-4}{1+e^{2\beta E}+e^{\beta E}(1-3\phi)} \right. \\ &\quad \left. + \frac{e^{\beta E}(9\phi^2-6\phi-1)-2}{1+e^{2\beta E}+e^{\beta E}(1+6\phi-9\phi^2)}\right). \end{aligned} \tag{21}$$

A comment regarding the color-dependent distribution function may be in order. Let us note that, for the color-dependent gluon distribution functions, the diagonal ones i.e., $f_{11}(E)$, $f_{22}(E)$, $f_{33}(E)$ are real, while the off-diagonal ones i.e., $f_{ij}(E)$ and $f_{ji}(E)$ are complex conjugates of each other. When the color sum is performed, the imaginary parts always cancel out, leading to the sum to be real. This cancellation of imaginary parts also always occurs for transport coefficients even with the color-dependent masses and leads to transport coefficients that are always real. The color-averaged distribution functions of the quark/antiquark are

$$f_{q/\bar{q}}(E) = \frac{1}{3}\sum_{a=1}^{3} f_a(E) = \frac{1}{3}\sum_{a=1}^{3} \tilde{f}_a(E) = \frac{\phi e^{-\beta E} + 2\phi e^{-2\beta E} + e^{-3\beta E}}{1 + 3\phi e^{-\beta E} + 3\phi e^{-2\beta E} + e^{-3\beta E}}. \quad (22)$$

Similar to the color-averaged distribution function $f_g(E)$, the color-averaged distribution function of the quark is real due to the cancellation of the imaginary parts of $f_1(E)$ and $f_3(E)$. It may be noted that for the pure gluon case, $\phi = 1$ in the confined phase and $\phi = 0$ in the deconfined phase. This leads to the gluon distribution function

$$f_g(E) = \frac{1}{e^{3\beta E} - 1} \quad (23)$$

in the confined phase and

$$f_g(E) = \frac{1}{e^{\beta E} - 1} \quad (24)$$

in the deconfined phase. In the presence of quarks, one does not have a rigorous order parameter for deconfinement; however, in the $\phi = 0$ case the color-averaged quark/antiquark distribution reduces to

$$f_{q/\bar{q}}(E) = \frac{1}{e^{3\beta E} + 1} \quad (25)$$

so that quarks are suppressed statistically. In the perturbative limit i.e., $\phi = 1$ it becomes

$$f_{q/\bar{q}}(E) = \frac{1}{e^{\beta E} + 1}. \quad (26)$$

The color-averaged distribution function of quarks/antiquarks as given in Eq. (22) is exactly the same as that in the PQM model within mean field approximation [42]. For the computation of Debye and thermal mass, we use double-line notation [55,56], which is convenient for large-$N_c$ calculations. For the $SU(N)$ gauge group, the generators $\lambda^A$ satisfy the following relation [46]:

$$\mathrm{Tr}(\lambda^A \lambda^B) = \frac{1}{2}\delta^{AB}, \quad (27)$$

where $A$ and $B$ are adjoint indices and take the values $A, B = 1, 2, 3, \ldots, N^2 - 1$. Each adjoint index can be denoted by a pair of fundamental indices. For double-line notation, the quantity that we need here is the projection operator; with adjoint indices it is written as

$$\mathcal{P}^{kl}_{mn} = \delta^k_m \delta^l_n - \frac{1}{N}\delta^{kl}\delta_{mn}. \quad (28)$$

In the calculation of quark and gluon self-energies, one needs the vertices for quark-antiquark-gluon ($q\bar{q}g$) interaction, which is proportional to the generators. In the double-line notation, the generators in the fundamental representation are written as

$$t^{ab}_{cd} = \frac{1}{\sqrt{2}}\mathcal{P}^{ab}_{cd}. \quad (29)$$

Here the upper pair $ab$ denotes the adjoint index, while the lower pair $cd$ denotes the components of this matrix in the fundamental representation. Similarly, the triple-gluon vertex is proportional to structure constants which in the double-line notation can be written as

$$f^{(kl,mn,ab)} = \frac{i}{\sqrt{2}}(\delta^{kn}\delta^{mb}\delta^{al} - \delta^{kb}\delta^{ml}\delta^{an}). \quad (30)$$

### A. Quark loop contribution to Debye mass

Generally, Debye mass ($m_D$) is defined through the pole of the effective propagator in the static limit i.e., $\omega = 0$, $\boldsymbol{p} \to 0$ and is related to the timelike component of gluon self-energy, $\Pi_{44}(\omega = 0, \boldsymbol{p} \to 0)$ [57]. It turns out that, in the presence of a static background field, apart from the usual $T^2$-dependent term similar to that in perturbative HTL calculations, there is an additional $T^3$-dependent contribution to the gluon self-energy. The latter component arises because the background field induces a color current which couples to the gluon. While the $T^2$-dependent term in $\Pi_{\mu\nu}$ is transverse [i.e., $P^\mu \Pi^{\mu\nu}(P) = 0$], the $T^3$-dependent term is not, and it spoils the transversality relation which is required for the gauge invariance. Therefore, one needs an additional contribution which may be of nonperturbative origin to the gluon self-energy to cancel such a term. Similar to Ref. [53], we assume that such a term exists and cancels this undesirable $T^3$ term. Under these assumptions, the Polyakov-loop-dependent resummed propagator can be written as [53]

$$D\mu\nu; abcd = P^L_{\mu\nu}\frac{k^2}{K^2}D^L_{abcd}(K) + P^T_{\mu\nu}D^T_{abcd}(K), \quad (31)$$

where $P^T_{\mu\nu} = g_{\mu i}(-g^{ij} - \frac{k^i k^j}{K^2})g_{j\nu}$ and $P^L_{\mu\nu} = -g_{\mu\nu} + \frac{k_\mu k_\nu}{K^2} - P^T_{\mu\nu}$, respectively, are the longitudinal and the transverse projection operators and are defined as

$$D^L_{\mu\nu;abcd}(K) = \left(\frac{i}{K^2 - F}\right)_{abcd}, \quad (32)$$

$$D^T_{\mu\nu;abcd}(K) = \left(\frac{i}{K^2 - G}\right)_{abcd}, \quad (33)$$

where

$$F = -2m^2\left(1 - \frac{x}{2}\ln\left(\frac{x+1}{x-1}\right)\right), \quad (34)$$

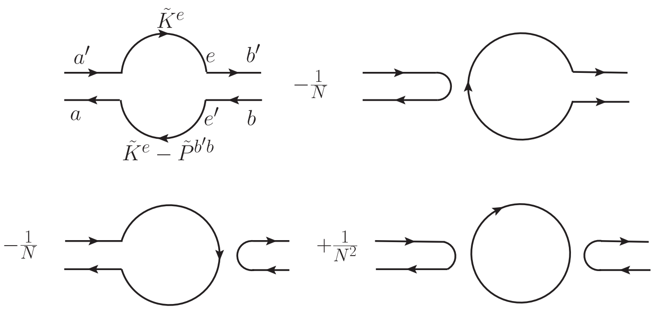


FIG. 1. Quark loop of gluon self-energy in double-line notation.

$$G = m^2\left(x^2 + \frac{x(1-x^2)}{2}\ln\left(\frac{x+1}{x-1}\right)\right), \tag{35}$$

where $x = \frac{k_0}{k}$ and $m^2 = (m^2)_{abcd}$ is the thermal mass of the gluon. Under the assumptions taken here, it is clear that the pole ($F$) of the longitudinal propagator can be related to the $\Pi_{44}$ component of gluon self-energy. Furthermore, in the static limit, this term can be defined as the Debye mass [46].

In this work, we shall focus only on the timelike component of the gluon self-energy with the assumption that the $T^3$-dependent term is canceled. For massless quarks, the Debye mass has already been computed in Ref. [46]. We include here the effect of the finite constituent quark mass in the quark loop contribution to the Debye mass. We work in the imaginary-time formalism of thermal field theory for evaluating the corresponding diagrams. In this formalism, because of the boundary conditions of imaginary time, the energy of a fermion $p_4$ is an odd multiple of $\pi T$, while that for a boson is an even multiple of $\pi T$. For calculating the Debye mass, we first evaluate the quark loop in the gluon self-energy, for which the corresponding diagram is shown in Fig. 1, where the loop momentum four-vector is written as $\tilde{K}^e_\mu = (K + \tilde{Q}_e)_\mu = (\omega_n + \tilde{Q}^e, \mathbf{k})$, with $\tilde{Q}_e = Q_e + \pi T$. In 't Hooft double-line notation, the polarization tensor can be written as

$$\Pi^q_{\mu\nu;b'baa'}(P,Q,m) = g^2 N_f t^{aa'}_{ee'} t^{bb'}_{e'e} \int \frac{d^4K}{(2\pi)^4} Tr_D \times [\gamma_\mu(\tilde{\not K}_e - \tilde{\not P}_{bb'})\gamma_\nu \tilde{\not K}_e + m^2\gamma_\mu\gamma_\nu] \times \Delta(K)\Delta(P-K), \tag{36}$$

where $aa', bb'(e,e')$ are color indices of gluons (quark/antiquark); $N_f$ is the quark flavor number; and $\Delta(K)^{-1} = (\omega_n + \tilde{Q}_e)^2 + \mathbf{k}^2 + m^2$; $\Delta(P-K)^{-1} = (\omega - \omega_n + Q_{bb'} - \tilde{Q}_e)^2 + (\mathbf{p}-\mathbf{k})^2 + m^2$ with $Q_{bb'} = Q_b - Q_{b'}$, $E_k = \sqrt{\mathbf{k}^2 + m^2}$, $E_q = \sqrt{(\mathbf{p}-\mathbf{k})^2 + m^2}$, $\omega_n = (2n+1)\pi T$, and $P_4 = \omega$. $Tr_D$ is the trace in Dirac space, and $Q_i$ is the diagonal matrix in color space, which is given as $Q_a = (-2\pi T q, 0, 2\pi T q)$, and $q$ is related to the Polyakov loop expectation value as given in Eq. (18). Here, we take the hard thermal loop (HTL) approximation and also assume that $m \ll T$. Thus, taking the HTL limit and the trace over Dirac space, Eq. (36) reduces to

$$\Pi^q_{\mu\nu;b'baa'}(P,Q,m) = g^2 N_f t^{aa'}_{ee'} t^{bb'}_{e'e} \int \frac{d^4K}{(2\pi)^4} [8(K+\tilde{Q}_e)_\mu (K+\tilde{Q}_e)_\nu - 4(K+\tilde{Q}_e)^2\delta_{\mu\nu} - 4m^2\delta_{\mu\nu}]\Delta(K)\Delta(P-K). \tag{37}$$

As we are interested in calculating the Debye mass, we need the timelike component ($\Pi_{44}$) of the gluon self-energy. So from here onwards, we shall proceed with this term. For this purpose, we write the integration in Eq. (37) as $\int \frac{d^4K}{(2\pi)^4} = T\sum_n \int \frac{d\mathbf{k}}{(2\pi)^3}$; $k_4 \equiv \omega_n = 2n\pi T$. Simplifying Eq. (37), we have

$$\Pi^q_{44;b'baa'}(P,Q,m) = 4g^2 N_f t^{aa'}_{ee'} t^{bb'}_{e'e} \int \frac{d\mathbf{k}}{(2\pi)^3} T\sum_n [(-2k^2 - m^2)\Delta(K)\Delta(P-K) + \Delta(P-K)]. \tag{38}$$

The frequency sums in Eq. (38) over discrete Matsubara frequencies are somewhat involved but can be performed routinely, leading to

$$T\sum_{n=-\infty}^{\infty}\Delta(K)\Delta(P-K) = \frac{1}{4E_kE_q}\left(\frac{f(E_q + iQ2 + i\omega) - f(E_k - iQ1)}{E_k - E_q + i(Q1+Q2+\omega)} + \frac{1 + f(E_k - iQ1) - f(E_q - iQ2 - i\omega)}{E_k + E_q - i(Q1+Q2+\omega)} + \frac{f(E_k + iQ1) - f(E_q - iQ2 - i\omega)}{E_q - E_k + i(Q1+Q2+\omega)} + \frac{1 + f(E_k + iQ1) - f(E_q + iQ2 + i\omega)}{E_k + E_q + i(Q1+Q2+\omega)}\right), \tag{39}$$

$$T\sum_{n=-\infty}^{\infty}\Delta(P-K) = -\frac{1 + f(E_q + iQ2 + i\omega) + f(E_q - iQ2 - i\omega)}{2E_q}, \tag{40}$$

where $Q2 = Q_{bb'} - \tilde{Q}_e$, $Q1 = \tilde{Q}_e$ and $f(E \pm iQ)$ is the Bose-Einstein distribution function. In Eqs. (39) and (40), the term which is independent of the distribution function is the vacuum contribution, which can be dropped when one considers the medium-dependent terms only. The first and third terms in Eq. (39) contribute to the $T^3$-dependent term. Such a term exists only in the presence of a background gauge field in the HTL approximations [46]. As mentioned earlier, this term spoils the transversality condition, and we shall not consider this undesirable contribution. Furthermore, the $T^2$-dependent contributions are given by the second and fourth terms of Eq. (39), as well as by the medium-dependent term in Eq. (40). In the static limit, the timelike component of the gluon self-energy can be written as

$$\Pi^q_{44;b'baa'}(Q,m)|_{(\omega=0,\boldsymbol{p}\to 0)} = -4g^2 N_f t^{aa'}_{ee'} t^{bb'}_{e'e}[2I_1(m,\tilde{Q}_e,Q_{bb'}-\tilde{Q}_e) + I_2(m,\tilde{Q}_e,Q_{bb'}-\tilde{Q}_e) + I_3(m,Q_{bb'}-\tilde{Q}_e)], \quad (41)$$

where

$$I_1(m,\tilde{Q}_e,Q_{bb'}-\tilde{Q}_e) = \frac{T^2}{16\pi^2}\int \frac{x^4 dx}{(x^2+y^2)^{\frac{3}{2}}}\Big(f(x,y,iq1)+f(x,y,-iq1)-f(x,y,iq2)-f(x,y,-iq2)\Big), \quad (42)$$

$$I_2(m,\tilde{Q}_e,Q_{bb'}-\tilde{Q}_e) = \frac{m^2}{16\pi^2}\int \frac{x^2 dx}{(x^2+y^2)^{\frac{3}{2}}}\Big(f(x,y,iq1)+f(x,y,-iq1)-f(x,y,iq2)-f(x,y,-iq2)\Big), \quad (43)$$

$$I_3(m,Q_{bb'}-\tilde{Q}_e) = \frac{T^2}{4\pi^2}\int \frac{x^2 dx}{\sqrt{x^2+y^2}}\Big(f(x,y,iq2)+f(x,y,-iq2)\Big), \quad (44)$$

where we have defined the dimensionless variables $x=\beta k$, $y=\beta m$, and $q1=\beta Q1$. Further, $f(x,y,iq)$'s are the Bose distribution functions in terms of these dimensionless variables as, e.g.,

$$f(x,y,iq) = \frac{1}{\exp(\sqrt{x^2+y^2}+iq)-1}. \quad (45)$$

Also note that although the distribution function is a complex quantity, the functions $I_1(m,\tilde{Q}_e,Q_{bb'}-\tilde{Q}_e)$, $I_2(m,\tilde{Q}_e,Q_{bb'}-\tilde{Q}_e)$, and $I_3(m,Q_{bb'}-\tilde{Q}_e)$ are real functions. With further simplification, $\Pi_{44}$ can be written as

$$\Pi^q_{44;b'baa'}(Q,m)|_{(\omega=0,\boldsymbol{p}\to 0)} = -g^2 N_f t^{aa'}_{e'e} t^{bb'}_{ee'} \frac{T^2}{4\pi^2}[2(\mathfrak{D}(q1,y)-\mathfrak{D}(q2,y)) + 4\mathfrak{F}(q2,y) + 2y^2\mathfrak{B}(Q2,y)], \quad (46)$$

where the dimensionless real functions $\mathfrak{D}$, $\mathfrak{F}$, and $\mathfrak{B}$ are

$$\mathfrak{D}(q,y) = \int \frac{x^4 dx}{(x^2+y^2)^{\frac{3}{2}}}\Big(f(x,y,iq)+f(x,y,-iq)\Big), \quad (47)$$

$$\mathfrak{B}(q,y) = \int \frac{x^2 dx}{(x^2+y^2)^{\frac{3}{2}}}\Big(f(x,y,iq)+f(x,y,-iq)\Big), \quad (48)$$

$$\mathfrak{F}(q,y) = \int \frac{x^2 dx}{\sqrt{x^2+y^2}}\Big(f(x,y,iq)+f(x,y,-iq)\Big). \quad (49)$$

In the limiting case of vanishing quark masses i.e., $y=0$ the function $\mathfrak{B}(q,y)$ does not contribute to $\Pi^q_{44}$, as it is multiplied by a $y^2$ term, while the functions $\mathfrak{D}(q,y=0)$ and $\mathfrak{F}(q,y=0)$ become equal and can be written in terms of Polylog functions $Li_2(z)$ as

$$\mathfrak{F}(q,y=0) = \mathfrak{D}(q,y=0) = \int dx x(f(x,y=0,iq)+f(x,y=0,-iq)) \equiv Li_2(iq) + Li_2(-iq). \quad (50)$$

The Polylog function $Li_2(z)$ can also be written in terms of Clausen functions $Cl_2(z)$; e.g.,

$$Li_2(i2\pi q) = \frac{\pi^2}{6}(1-6q+6q^2) + iCl_2(2\pi q), \quad (51)$$

which has been used in Ref. [46]. In the present investigation, however, we will keep the effect of masses in Eqs. (47), (48), and (49) and integrate it numerically to estimate the Debye mass. Generators appearing on the right side of Eq. (46) can be simplified by using projection operators, so that the product of two generators becomes

$$t^{aa'}_{e'e}t^{bb'}_{ee'} = \frac{1}{2}\left[\delta^{be}\delta^{b'e'}\delta^{a'e}\delta^{ae'} - \frac{1}{N}(\delta^{bb'}\delta^{ee'}\delta^{a'e}\delta^{ae'} + \delta^{be}\delta^{b'e'}\delta^{aa'}\delta^{e'e}) + \frac{1}{N^2}\delta^{bb'}\delta^{ee'}\delta^{aa'}\delta^{e'e}\right]. \tag{52}$$

Note that $\Pi_{44}$ depends on the color of the quark and gluon and has $a, b, a', b'$ as free color indices. So we need to sum over other repeated color indices (i.e., $e$, $e'$), which can be done by contracting the color indices of Eq. (52) with those of Eq. (46). Using Eq. (52) along with Eq. (46) and summing over contracted color indices, gluon self-energy can be written as

$$\begin{aligned}\Pi^q_{44;b'baa'}(Q,m)|_{(\omega=0,\boldsymbol{p}\to 0)} = -g^2 N_f\frac{T^2}{4\pi^2}\Big[&\delta_{ab}\delta_{a'b'}(\mathfrak{D}(\tilde{Q}_b,y) - \mathfrak{D}(\tilde{Q}_{b'},y) + 2\mathfrak{F}(\tilde{Q}_{b'},y) + y^2\mathfrak{B}(\tilde{Q}_{b'},y))\\ &-\frac{1}{N}(\mathfrak{D}(\tilde{Q}_{b'},y) + \mathfrak{D}(\tilde{Q}_{a'},y) + \mathfrak{F}(\tilde{Q}_{b'},y) + \mathfrak{F}(\tilde{Q}_{a'},y) + 2y^2\mathfrak{B}(\tilde{Q}_{a'},y)\\ &+2y^2\mathfrak{B}(\tilde{Q}_{b'},y))\delta_{aa'}\delta_{bb'} + \frac{1}{N^2}\sum_e(\mathfrak{D}(\tilde{Q}_e,y) + \mathfrak{F}(\tilde{Q}_e,y)\\ &+2y^2\mathfrak{B}(\tilde{Q}_e,y))\delta_{aa'}\delta_{bb'}\Big].\end{aligned} \tag{53}$$

### B. Gluon contribution to Debye mass

The gluon loop contribution to the gluon self-energy has already been evaluated in Ref. [46]. For the sake of completeness, we recapitulate the results here. The gluon loop diagram with a trigluon vertex is shown in Fig. 2. In the HTL approximation, the sum of the gluon loop, four-gluon vertex, and ghost loop contributions to the gluon self-energy can be written as

$$\begin{aligned}\Pi^{gl}_{\mu\nu;b'baa'}(P,Q) &= g^2 f^{(b'b,ee',gh)}f^{(aa',e'e,hg)}\\ &\times\int\frac{d^4K}{(2\pi)^4}[4K_{\mu e'e}K_{\nu e'e} - 2K^2_{e'e}\delta_{\mu\nu}]\\ &\times\Delta(K)\Delta(P-K).\end{aligned} \tag{54}$$

As explained earlier, the timelike component of the self-energy is needed for the Debye mass, which can be written as

$$\begin{aligned}&\Pi^{gl}_{44;b'baa'}(P,Q)\\ &= g^2 f^{(b'b,ee',gh)}f^{(aa',e'e,hg)}\int\frac{d\mathbf{k}}{(2\pi)^3}\sum_n T[2\Delta(P-K)\\ &-4k^2\Delta(K)\Delta(P-K)],\end{aligned} \tag{55}$$

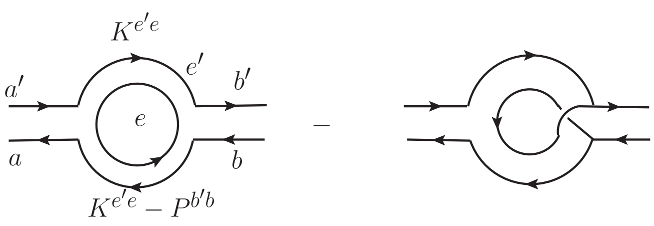


FIG. 2. Gluon loop in gluon self-energy in double-line notation.

where $\Delta(K)^{-1} = (\omega_n + Q_{e'e})^2$ and $\Delta(P-K)^{-1} = (\omega - \omega_n + Q_{b'b} - Q_{e'e})^2 + E_q^2$. Here $Q1 = Q_{e'e}$ and $Q2 = Q_{b'b} - Q_{e'e}$. Similarly to the quark loop, we shall not consider the $T^3$-dependent term here, and the summation over discrete Matsubara frequencies is the same as in Eqs. (39) and (40). Using these summations and taking the static limit, the $T^2$-dependent contribution to gluon self-energy can be written as

$$\begin{aligned}\Pi^{gl}_{44;b'baa'}(Q)|_{(\omega=0,\boldsymbol{p}\to 0)} = -&\frac{g^2T^2}{4\pi^2}f^{(b'b,ee',gh)}f^{(aa',e'e,hg)}\\ &\times[3\mathfrak{H}(Q_{b'b} - q_{e'e}) + \mathfrak{H}(Q_{e'e})],\end{aligned} \tag{56}$$

where

$$\begin{aligned}\mathfrak{H}(Q) &= \int xdx(f(x,iq) + f(x,-iq))\\ &\equiv Li_2(iq) + Li_2(-iq).\end{aligned} \tag{57}$$

The same as in the case of the quark loop, for gluon loops, gluon self-energy depends on the color of the gluon, and these color indices are free. Other repeated color indices can be summed by using Eq. (30) for a structure constant. Thus, Eq. (56) becomes

$$\begin{aligned}&\Pi^{gl}_{44;b'baa'}(Q)|_{(\omega=0,\boldsymbol{p}\to 0)}\\ &= \frac{g^2T^2}{8\pi^2}[4(\mathfrak{H}(Q_{ba}) + \mathfrak{H}(Q_{ab}))\delta^{b'b}\delta^{a'a}\\ &\quad - 2(3\mathfrak{H}(Q_{be}) + \mathfrak{H}(Q_{b'e}))\delta^{a'b'}\delta^{ab}].\end{aligned} \tag{58}$$

To get the total Debye mass, we need to add both of the contributions which are given in Eqs. (53) and (58). Taking both the contributions into account, the Debye mass can be given as

$$(m_D^2)_{b'baa'} = -\Pi^q_{44;b'baa'}(m)|_{(\omega=0,\boldsymbol{p}\to 0)} - \Pi^{gl}_{44;b'baa'}(Q)|_{(\omega=0,\boldsymbol{p}\to 0)}, \tag{59}$$

leading to

$$\begin{aligned}(m_D^2)_{b'baa'} = \frac{g^2T^2}{4\pi^2}\Bigg[N_f\Bigg(&\delta_{ab}\delta_{a'b'}(\mathfrak{D}(\tilde{Q}_b,y) - \mathfrak{D}(\tilde{Q}_{b'},y) + 2\mathfrak{F}(\tilde{Q}_{b'},y) + y^2\mathfrak{B}(\tilde{Q}_{b'},y))\\ &-\frac{1}{N}(\mathfrak{D}(\tilde{Q}_{b'},y) + \mathfrak{D}(\tilde{Q}_{a'},y) + \mathfrak{F}(\tilde{Q}_{b'},y) + \mathfrak{F}(\tilde{Q}_{a'},y) + 2y^2\mathfrak{B}(\tilde{Q}_{a'},y) + 2y^2\mathfrak{B}(\tilde{Q}_{b'},y))\delta_{aa'}\delta_{bb'}\\ &+\frac{1}{N^2}\sum_e(\mathfrak{D}(\tilde{Q}_e,y) + \mathfrak{F}(\tilde{Q}_e,y) + 2y^2\mathfrak{B}(\tilde{Q}_e,y))\delta_{aa'}\delta_{bb'}\Bigg) + (3\mathfrak{H}(Q_{be}) + \mathfrak{H}(Q_{b'e}))\delta^{ab}\delta^{a'b'}\\ &-(2(\mathfrak{H}(Q_{ba}) - \mathfrak{H}(Q_{ab})))\delta^{b'b}\delta^{a'a}\Bigg].\end{aligned} \tag{60}$$

As the Debye mass is color dependent, one needs to sum the contributions from all the colors and then average over the number of colors to get the total Debye mass; i.e.,

$$\bar{m}_D^2 = \sum_{abcd}\frac{(m_D^2)_{abcd}}{N^4}. \tag{61}$$

In the large-$N$ limit (i.e., neglecting $1/N$ terms in Eq. (60)), the Debye mass is diagonal, and its components can be written in the limit quark mass $m = 0$ as

$$(m_D^2)_1 = (m_D^2)_3 = \frac{g^2T^2}{6}(6 + N_f - 36q + (60 - 12N_f)q^2), \tag{62}$$

$$(m_D^2)_2 = \frac{g^2T^2}{6}(N_f + 6(1-2q)^2). \tag{63}$$

which is same as was derived in Ref. [46]. It is easy to check that, in the limit $Q = 0$ and $m = 0$, the Debye mass as written in Eq. (60) reduces to its familiar HTL limit, given as

$$(m_D^2)_{abcd} = \frac{g^2T^2}{3}\left(N_c + \frac{N_f}{2}\right)\mathcal{P}_{abcd}. \tag{64}$$

In our calculation for the heavy quark transport coefficients, however, we will use the color-averaged Debye mass as given in Eq. (61).

### C. Light quark thermal mass

In the double-line notation, the standard diagram of one-loop quark self-energy is shown in Fig. 3, where $a$ and $a'$, respectively, are the color indices for incoming and outgoing quarks. It is expected that similar to the gluon self-energy, the quark self-energy also depends on the colors of incoming and outgoing quarks, and in the presence of a background gauge field, the same can be written as

$$\begin{aligned}\Sigma(P,Q,m)_{a'a} &= g^2(t^{de})_{a'b}\mathcal{P}_{defg}(t^{fg})_{ba}\\ &\quad\times\int\frac{d^4K}{(2\pi)^4}\frac{\gamma^\mu(m - \tilde{\not{K}}_b)\gamma_\mu}{(\tilde{P}_{a'} - \tilde{K}_b)^2(\tilde{K}_b^2 + m^2)},\end{aligned} \tag{65}$$

where $g$ is the coupling constant, $\tilde{K}_b = K + \tilde{Q}_b$ is the quark momentum, and $\tilde{P}_{a'} - \tilde{K}_b = P - K + \tilde{Q}_a - \tilde{Q}_b$ is the gluon momentum. To solve the integration in Eq. (65), let us first write $\int\frac{d^4K}{(2\pi)^4} = \sum_n\int\frac{d\mathbf{k}}{(2\pi)^3}$; $k_4 \equiv \omega_n = 2n\pi T$ and perform a Matsubara frequency sum. There are two types of terms where one needs to perform frequency summation. One is similar to Eq. (39) with the product of two propagators, $\sum\Delta(K)\Delta(P-K)$ (arising from the term proportional to $m$), and another is $\sum\omega_n\Delta(K)\Delta(P-K)$ (arising from the $\tilde{\not{K}}_b$ term). The latter one can be written as

$$\begin{aligned}T\sum_n\omega_n\Delta(K)\Delta(P-K) = \frac{i}{4E_q}\Bigg(&\frac{f(E_q + iQ2 + i\omega) - f(E_k - iQ1)}{E_k - E_q - i(Q1 + Q2 + \omega)} + \frac{1 + f(E_k - iQ1) + f(E_q - iQ2 - i\omega)}{E_k + E_q - i(Q1 + Q2 + \omega)}\\ &+\frac{f(E_q - iQ2 - i\omega) - f(E_k + iQ1)}{E_k - E_q + i(Q1 + Q2 + \omega)} + \frac{1 + f(E_q + iQ2 + i\omega) + f(E_k + iQ1)}{E_k + E_q + i(Q1 + Q2 + \omega)}\Bigg).\end{aligned} \tag{66}$$

We take the HTL approximation and evaluate only $T^2$-dependent terms in quark self-energy. We note here that, unlike gluon self-energy, one does not get any extra term different in structure as compared to the usual perturbative HTL approximation for the quark self-energy. The leading contribution arises from the terms having $E_q - E_k$ in the denominators of Matsubara frequency sums, and in Eq. (66) comes from the first and the third terms. Simplifying Eq. (65) with Eqs. (39) and (66), quark self-energy becomes

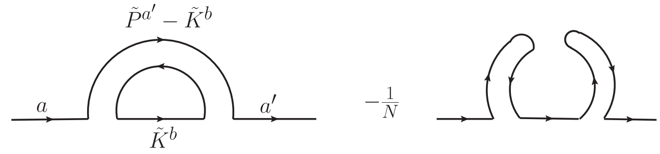


FIG. 3. One-loop quark self-energy diagram in double-line notation.

$$\Sigma(P,Q,m)_{a'a} = g^2 \mathcal{P}_{a'b,ba}\Bigg(m\int\frac{d\mathbf{k}}{(2\pi)^3}\frac{1}{4E_kE_q}\Bigg[\frac{f(E_q-iQ2)+f(E_q+iQ2)}{P_a.\hat{K}} - \frac{f(E_k+iQ1)+f(E_k-iQ1)}{P_a.\hat{K}}\Bigg] + \int\frac{\hat{\not{K}}d^3k}{E_k(2\pi)^3}\Bigg[\frac{f(E_k+iQ2)-f(E_q-i(Q1+\omega))}{P_a.\hat{K}} - \frac{f(E_q+i(Q1+\omega))-f(E_k-iQ2)}{P_a.\hat{K}}\Bigg]\Bigg). \quad (67)$$

In the above equation, we have used HTL approximation so that $E_q - E_k \approx -\frac{\boldsymbol{P.k}}{E_k}$, $f(E_k - iQ) \approx f(E_q - iQ)$ and $e^{\frac{i\omega}{T}} \simeq 1$. Here $Q1 = \tilde{Q}_b$, $Q2 = Q_{a'} - Q_b$, and $\hat{K} = (i, \hat{k})$. After simplifying Eq. (67) further, it can be written as

$$\Sigma(P,Q,m)_{a'a} = \frac{g^2T^2}{8\pi^2}\sum_{b=1}^{3}\mathcal{P}_{a'b,ba}\left([\mathfrak{F}(q2,y)-\mathfrak{F}(q1,y)]\int\frac{d\Omega}{4\pi}\frac{\hat{\not{K}}}{P_a.\hat{K}} + \frac{m}{T}(\mathfrak{I}(q2,y)-\mathfrak{I}(q1,y))\int\frac{d\Omega}{4\pi}\frac{1}{P_a.\hat{K}}\right), \quad (68)$$

where as before, $y = \beta m$, $q1 = \beta Q1$; $\mathfrak{F}(q)$ is the same as given in Eq. (49), and $\mathfrak{I}$ is given as

$$\mathfrak{I}(q,y) = \int\frac{x^2dx}{x^2+y^2}(f(x,y,-iq)+f(x,y,iq)). \quad (69)$$

It is easy to see that to estimate the quark thermal mass from its self-energy, one needs to sum over colors in Eq. (68), keeping $a$ and $a'$ open indices. After performing this color sum, quark self-energy reduces to

$$\Sigma(P,Q,m)_{a'a} = \frac{g^2T^2}{8\pi^2}\delta_{a'a}\Bigg(\Bigg[\sum_{b=1}^{3}(\mathfrak{F}(q_{a'b},y)-\mathfrak{F}(\tilde{q}_b,y)) - \frac{1}{3}(\mathfrak{F}(0,y)-\mathfrak{F}(\tilde{q}_a,y))\Bigg]\int\frac{d\Omega}{4\pi}\frac{\hat{\not{K}}}{P_a.\hat{K}} + \frac{m}{T}\Bigg[\sum_{b=1}^{3}(\mathfrak{I}(q_{a'b},y)-\mathfrak{I}(\tilde{q}_b,y)) + \mathfrak{I}(0,y)-\mathfrak{I}(\tilde{q}_a,y)\Bigg]\int\frac{d\Omega}{4\pi}\frac{1}{P_a.\hat{K}}\Bigg). \quad (70)$$

In the HTL approximation, the effective fermion mass (thermal mass) can be written as [58]

$$4m_{th}^2 = \mathrm{Tr}(\not{P}\Sigma(P)). \quad (71)$$

From Eqs. (71) and (70), the color-dependent quark thermal mass a function of the Polyakov loop parameter $q$ can be written as

$$m_{a'}^2 = \frac{g^2T^2}{8\pi^2}\left(\sum_{b=1}^{3}(\mathfrak{F}(Q_{a'b},y)-\mathfrak{F}(\tilde{Q}_b,y)) - \frac{1}{3}(\mathfrak{F}(0,y)-\mathfrak{F}(\tilde{Q}_{a'},y))\right). \quad (72)$$

In the limit of vanishing quark mass, using Eq. (50), it is easy to show that

$$m_a^2 = \frac{g^2T^2}{6}\left(1+\frac{3}{2}q_a+\frac{7}{2}q_a^2\right). \quad (73)$$

In the subsequent calculations that follow, however, we keep the quark mass dependence as in Eq. (72). Similarly to Eq. (61), one can define a color-averaged quark thermal mass as

$$m_{th}^2 = \sum_{a=1}^{3}\frac{m_a^2}{3}, \quad (74)$$

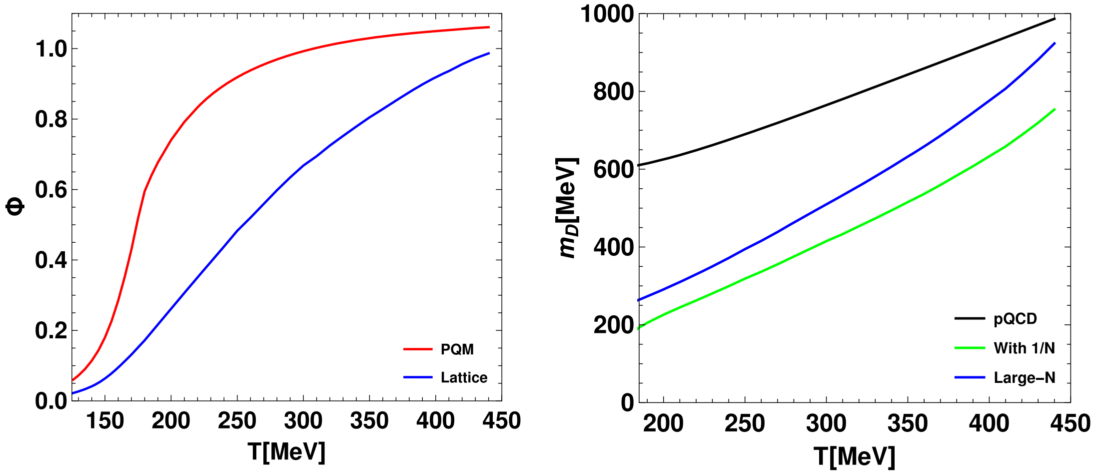


FIG. 4. *Left panel:* Polyakov loop value as a function of temperature. The red curve is from the PQM model [42]. The blue curve is from the lattice results of Ref. [59]. *Right panel:* Debye mass ($m_D$) as a function of temperature. The black curve corresponds to pQCD hard thermal loop calculations [57]. The blue curve corresponds to the large-$N$ limit for $m_D$ as given in Eq. (60). The green curve correspond to taking all the terms in Eq. (60) for $N = 3$. Here the Polyakov loop is taken from lattice data [59].

so the total quark mass becomes

$$m_q = m + m_{th}. \tag{75}$$

Thus, the color-averaged Debye mass for the gluons and the color-averaged thermal mass for quarks as given by Eqs. (61) and (74) depend upon the Polyakov loop parameter.

For the Polyakov loop parameter, we adopt here two approaches. First, we estimate the same from a phenomenological two-flavor PQM model [37,42]. The salient features of the model and the parameters taken in the model are discussed in Appendix A. With this parametrization, the critical temperature for the crossover transition $T_c \approx 176$ MeV. We also take the Polyakov loop parameter from lattice simulations as in Ref. [59]. The variation of the Polyakov loop with temperature ($T$) is shown on the left of Fig. 4. Clearly, compared to the lattice simulations, the Polyakov loop parameter $\phi$ in the PQM model shows a sharper rise and reaches its asymptotic value $\phi = 1$ at a temperature around 320 MeV. On the other hand, in the lattice simulations, this happens at a much higher temperature. This means that the nonperturbative effects are significant up to temperatures as high as 400 MeV in the lattice. However, in PQM, these effects are significant only for temperatures up to around 320 MeV. On the right side of Fig. 4, the Debye mass as a function of temperature

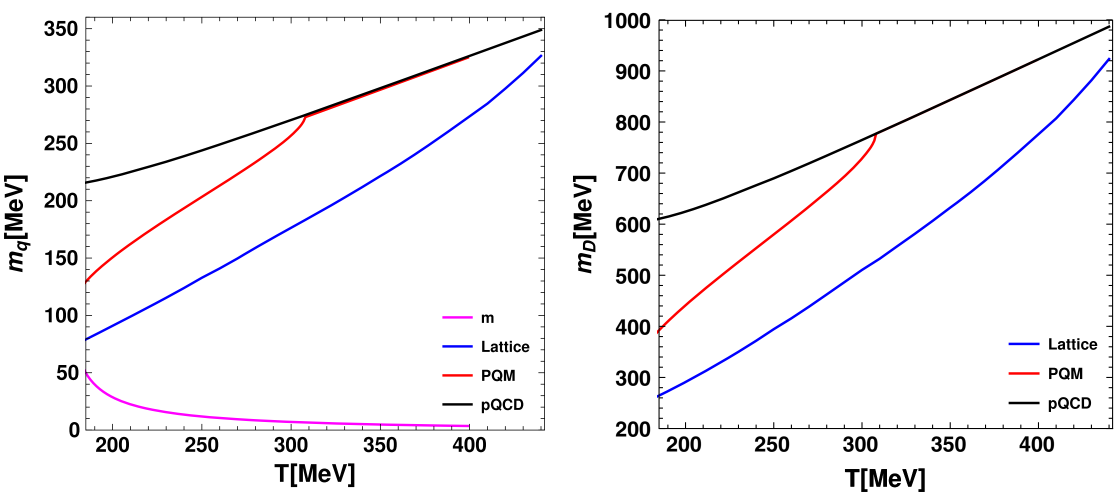


FIG. 5. *Left panel:* Quark masses as a function of temperature. The bottommost curve (magenta) shows the constituent quark mass estimated in the PQM model. The topmost curve (black) shows the perturbative HTL estimate of the quark thermal mass [57]. The red curve shows the temperature dependence of the quark thermal mass [Eq. (74)] with the Polyakov loop taken from PQM model calculations. The blue curve shows the thermal mass of the quark [Eq. (74)] using the Polyakov loop from lattice simulations [59]. *Right panel:* Debye mass as a function of temperature in the leading order in $N$ of Eq. (60). The blue curve correspond to the Polyakov loop value taken from lattice data [59], while the red curve corresponds to the Polyakov loop value taken from the PQM model.

is shown. Here the black curve corresponds to the Debye mass in pQCD, while the blue and the green curves are in the presence of the Polyakov loop. The blue curve corresponds to the large-$N$ limit [i.e., dropping $1/N$ terms in Eq. (53)]. On the other hand, the green curve corresponds to including the $1/N$ terms in Eq. (53). Clearly, the large-$N$ limit approaches the perturbative limit faster compared to the one including $1/N$ terms for the Debye mass.

For the light quarks, different contributions to the masses as a function of temperature ($T$) are shown on the left side of Fig. 5. The red and blue curves correspond to quark thermal masses ($m_{th}$) as given in Eq. (74) and evaluated in the HTL approximation in the presence of a background gauge field. The red curve corresponds to the Polyakov loop value taken from the PQM model, while the blue curve corresponds to the same taken from lattice simulations. The HTL perturbative QCD thermal mass as in Ref. [57] is shown by the black curve. Clearly, with lattice values of the Polyakov loop, thermal masses approach the perturbative results at a much higher temperature, while with values taken from PQM, the perturbative limit is reached at a relatively lower temperature around 320 MeV. It ought to be mentioned that beyond 330 MeV, the $\phi$ value is larger than 1, in which case $q$ becomes imaginary. We have taken here the real part of $q$ for estimating the thermal masses. Beyond temperature 330 MeV, the real part of $q$ vanishes, which leads to the perturbative limit. As compared to the PQM model, the color-averaged thermal mass is smaller for the Polyakov loop expectation value taken from the lattice simulation. This is because, with the smaller value of $\phi$, statistical distribution functions are suppressed more. The magenta curve is the constituent quark mass estimated in the PQM model. The right side of Fig. 5 shows the behavior of the color-averaged Debye mass in the large-$N$ limit of Eq. (60). The red and the blue curves correspond to the masses with Polyakov loop values taken from the PQM and lattice simulations, respectively. The Debye mass is smaller as compared to the perturbative QCD Debye mass, and this suppression is more when $\phi$ is taken from the lattice simulations. The reason for this is the same as that for the case of quark thermal mass. In the estimation of the transport coefficients, we shall use the Debye mass and thermal masses of quarks as in Eq. (75). It is clear that the nonperturbative effects which are in the distribution function and the masses of quarks and gluons can significantly affect these transport coefficients as compared to the perturbative QCD.

## IV. RESULTS AND DISCUSSIONS

With the thermal mass of the quarks and the Debye mass as computed in the background of a nontrivial Polyakov loop, we next numerically compute the drag and diffusion coefficients using Eq. (15). For the heavy quark elastic interaction with the light quarks and gluons, $qQ \to qQ$ and $gQ \to gQ$ scattering processes are considered where $Q$ stands for a heavy quark, $q$ stands for a light quark, and $g$ stands for the gluon. In the case of massless light quarks and gluons, the leading-order (LO) matrix elements for $qQ \to qQ$ and $gQ \to gQ$ scattering have been calculated in Refs. [45,60]. These pQCD cross sections have to be supplemented by the value of the coupling constant and the Debye screening mass, which is needed to shield the divergence associated with the $t$-channel diagrams to compute the heavy quark transport coefficients. For massive light quarks and gluons, the calculation of the scattering matrix, $\mathcal{M}_{(q,g)+Q\to(q,g)+Q}$, is performed considering the leading-order (LO) diagram with massive quark and gluon propagators for $gQ \to gQ$ and a massive gluon propagator for $qQ \to qQ$ scatterings [21,23]. Within the matrix model, the scattering amplitudes are summarized in Appendix B. Similarly to previous work [21,23], a massive gluon propagator for $qQ \to qQ$ and the $t$ channel of $gQ \to gQ$ is used. We estimate the transport coefficients for the charm quark, whose mass is taken as $m_C = 1.27$ GeV. Here we use the two-loop running coupling constant given as [61]

$$\alpha_s = \frac{1}{4\pi}\left(\frac{1}{2\beta_0 \ln(\frac{\pi T}{\Lambda}) + \frac{\beta_1}{\beta_0}\ln(2\ln(\frac{\pi T}{\Lambda}))}\right), \tag{76}$$

where

$$\beta_0 = \frac{1}{16\pi^2}\left(11 - \frac{2N_f}{3}\right), \tag{77}$$

$$\beta_1 = \frac{1}{(16\pi^2)^2}\left(102 - \frac{38N_f}{3}\right), \tag{78}$$

with $\Lambda = 260$ MeV and $N_f = 2$.

We evaluate the drag and diffusion coefficients of heavy quarks in QGP with Polyakov loop values from two different models. In one case, the Polyakov loop value—and hence the Debye mass and thermal masses—has been taken from PQM calculation as an input to compute the heavy quark transport, and we label it as PQM. In the other case, the Polyakov loop value has been taken from the lattice simulations, and hence, we label it as lattice in the following discussions.

The temperature variation of the drag coefficient has been shown in Fig. 6 for charm quark interaction with light quarks and gluons for a given momentum ($p = 0.1$ GeV) obtained for both PQM and lattice Polyakov loop values.

We obtain quite a mild temperature dependence of the heavy quark drag coefficient for the case of PQM. However, in the lattice case, we obtain a quite stronger temperature dependence of the heavy quark drag coefficient than the one with PQM. We notice that the drag coefficient obtained with PQM input is larger at low temperature than the one obtained with lattice inputs, whereas the trend is opposite at high temperature. This is mainly because of the

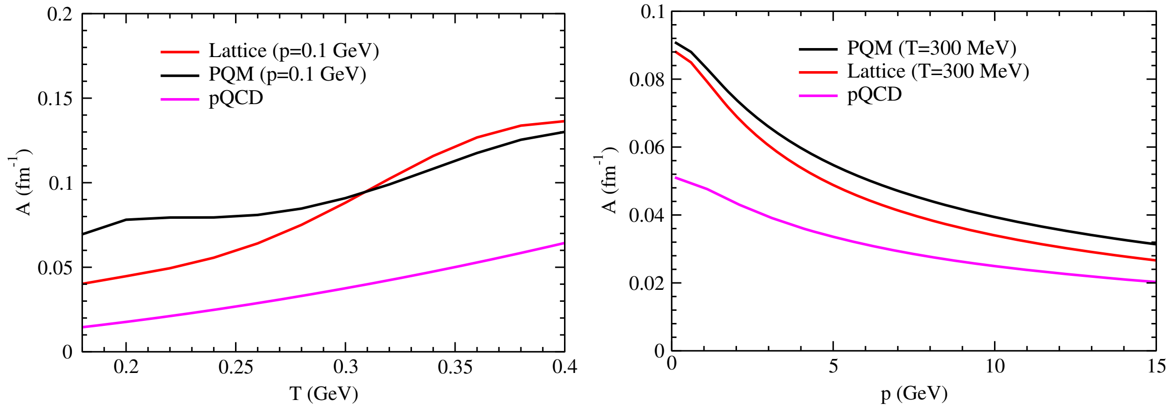


FIG. 6. Variation of drag coefficients ($A$) with temperature (left) for momentum $p = 100$ MeV, and with momentum (right) for temperature $T = 300$ MeV.

interplay between the Debye mass and the Polyakov loop value obtained within both the models. In the same plot, for comparison, we have also included results for the drag coefficient obtained within the standard LO pQCD calculations with a constant coupling ($\alpha_s = 0.2$) to display the nonperturbative effects arising from the nontrivial Polyakov loop and chiral condensate on the HQ drag coefficient.

A smaller value of the Polyakov loop, as shown on the left side of Fig. 4 in the lattice case, reduces the magnitude of the drag coefficients at low temperature. However, at high temperature, a smaller Debye mass, as shown in Fig. 5 obtained with lattice input, enhances the magnitude of heavy quark drag coefficients. Hence, at low temperature, the Polyakov loop value plays the dominant role (e.g., at $T = 180$ MeV, the Polyakov loop values obtained with the two models differ by a factor of about 2), whereas at high temperature, the Debye mass plays the dominant role (e.g., at $T = 300$ MeV, the difference between the Polyakov loop values obtained with the two cases is reduced significantly) for the behavior of the drag coefficient.

We observed that the temperature dependence of the heavy quark drag coefficient obtained with the PQM Polyakov loop value is quite consistent with the results obtained with other quasiparticle models [20,23] and the $T$-matrix approach [18]. It is important to mention that the temperature dependence of the drag coefficient plays a significant role [20] in describing the heavy quarks $R_{AA}$ and $v_2$ simultaneously, which is a challenge to almost all the models on heavy quark dynamics. A constant or weak temperature dependence of the drag coefficient is an essential ingredient for reproducing the heavy quarks $R_{AA}$ and $v_2$ simultaneously, whereas in pQCD the drag coefficient increases with temperature.

The momentum variation of the drag coefficient has been shown in the right panel of Fig. 6 for charm quark interaction with light quarks and gluons obtained with the PQM and lattice Polyakov loop values. We observe a strong momentum dependence of heavy quark drag coefficient as compared to the same estimated within pQCD [7,21]. This is mainly due to the inclusion of nonperturbative effects through the Polyakov loop background. At $T = 300$ MeV, the drag obtained with the PQM Polyakov loop (at $p = 0.1$ GeV) is marginally larger than the drag obtained with the lattice Polyakov value. Hence, the

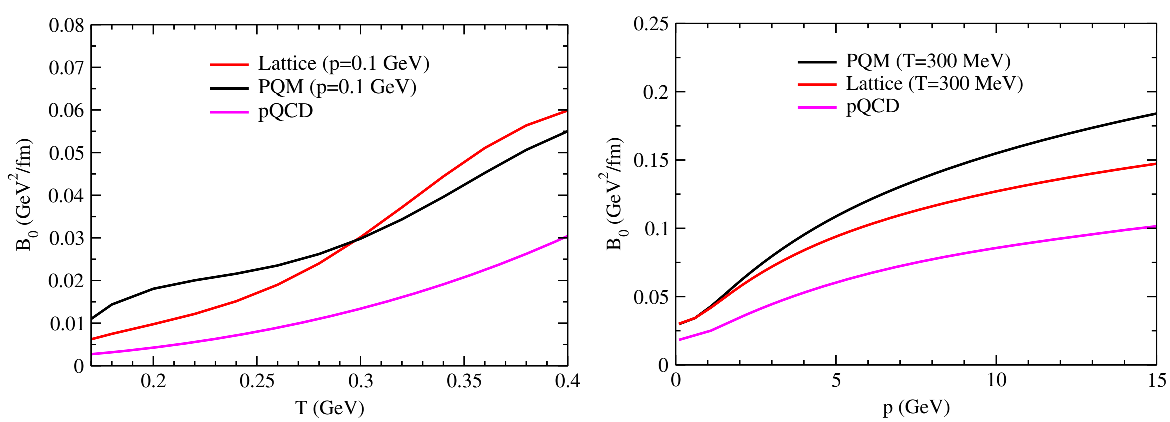


FIG. 7. Variation of diffusion coefficients ($B_0$) with temperature (left) for momentum $p = 100$ MeV, and with momentum (right) for temperature $T = 300$ MeV.

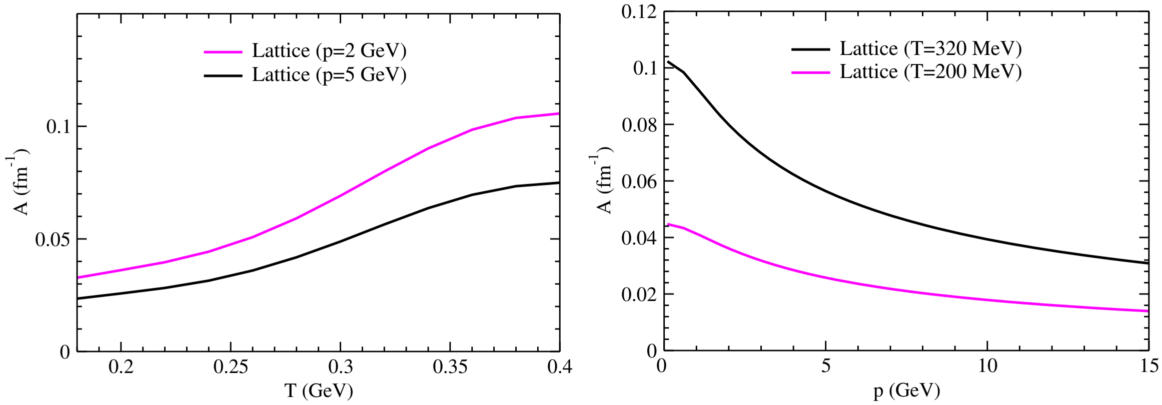


FIG. 8. Variation of drag coefficients ($A$) with temperature (left) for different values of momentum, and with momentum (right) for different values of temperature. The Polyakov loop value is taken from the lattice data [59].

momentum variation of drag coefficients obtained with inputs from PQM is marginally larger than that obtained with inputs from lattice simulation in the entire momentum range considered here.

In Fig. 7, the heavy quark diffusion coefficient $B_0$ has been displayed as a function of temperature obtained with input parameters from PQM and lattice. The diffusion coefficients increase with temperature for both the cases, as it involves the square of the momentum transfer. In terms of magnitude, the diffusion coefficient obtained in both the cases follows a similar trend of drag coefficient due to the same reason (i.e., interplay between the Debye mass and Polyakov loop value). In the same plot, we have also included the diffusion coefficient obtained within the standard LO pQCD calculation for a constant coupling to highlight the nonperturbative features arising from nontrivial Polyakov loop and chiral condensates.

The momentum variation of the diffusion coefficient has been shown in Fig. 7 for charm quark interaction with light quarks and gluons for the same values of the Polyakov loop. Similar to the drag coefficient, the diffusion coefficient also shows the same trend, with PQM having larger values then that from the lattice as a function of momentum. A stronger suppression of the distribution function at high momentum in the lattice Polyakov loop than that from the PQM also plays a marginal role in the momentum variation of heavy quark drag and diffusion coefficients obtained.

To understand the temperature dependence of the transport coefficients, we plot the temperature variation of the drag coefficient in Fig. 8 at different momenta obtained with Polyakov loop values from lattice simulations. We obtain an almost similar temperature dependence of the heavy quark drag coefficient, with both momenta having larger magnitude at $p = 2$ GeV than at $p = 5$ GeV. In Fig. 9, we have depicted the temperature variation of the diffusion coefficient at different momenta for the same values of the Polyakov loop. As expected, the magnitude of the diffusion coefficient is larger at $p = 5$ GeV than $p = 2$ GeV, having similar temperature variation for both the momenta.

In Fig. 8, we have shown the variation of drag coefficient with momentum at different temperatures obtained with the lattice inputs. We observe a larger magnitude of the drag coefficient at $T = 320$ MeV than at $T = 200$ MeV, but the

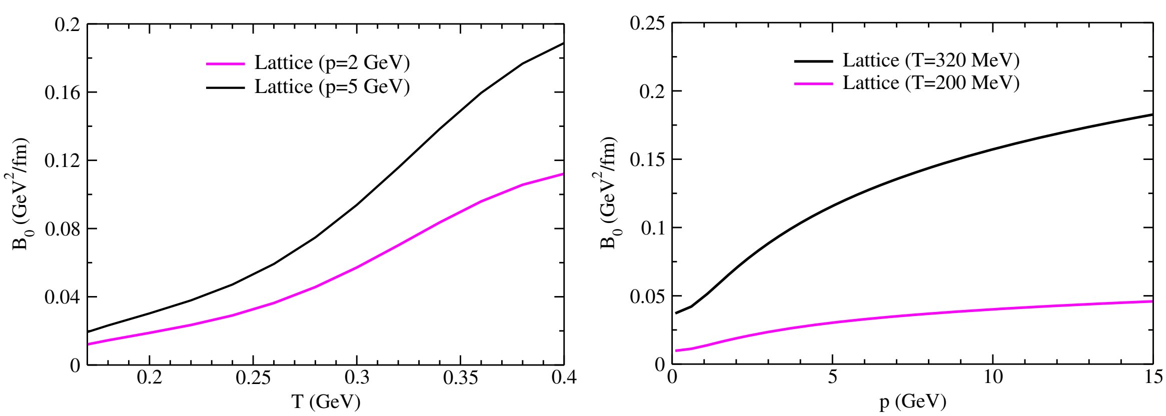


FIG. 9. Variation of diffusion coefficients ($B_0$) with temperature (left) for different values of momentum, and with momentum (right) for different values of temperature. The Polyakov loop value is taken from the lattice data [59].

momentum variation is similar at both temperatures. Momentum variation of the diffusion coefficient has also been depicted in Fig. 9 at different temperatures. At both momenta, the diffusion increases with temperature, having a larger magnitude at $T = 320$ MeV than at $T = 200$ MeV.

It is worth mentioning here that nonperturbative effects from a different perspective have been investigated recently in Refs. [62–64] and employed to calculate the transport coefficients [64]. The method here consisted of using a $T$ matrix with an in-medium potential for the heavy quarks. This potential is constrained by the heavy quark free energy from the lattice data. The lattice heavy quark free energy is directly related to the Polyakov loop, and hence is correlated with the strength of the confining potential. Therefore, it is nice to see that the behavior of the drag coefficient being rather flat with regard to temperature dependence, whereas the diffusion coefficient has a strong temperature dependence as observed here, was also observed in Ref. [64]. This consistency suggests the possible existence of model-independent correlation between the Polyakov loop and the heavy quark transport coefficients.

## V. SUMMARY

In this work, we have computed the heavy quark drag and diffusion coefficients in QGP including nonperturbative effects via a Polyakov loop background. In order to incorporate these effects, we first calculate the quark and gluon thermal masses, also taking the quark constituent mass into account. We found that for temperatures below 300 MeV, the quark thermal mass and gluon Debye mass start deviating from their perturbative values. This effect is significant for even higher temperatures when Polyakov values are taken from the lattice simulations. This decrease in the Debye mass of the gluon and the thermal mass of light quarks is due to color suppression manifested in the quark and gluon distribution functions in the presence of a background Polyakov loop field. In the calculation of the HQ diffusion coefficient, the distribution function of the light quark and the Debye mass play complimentary roles. While the distribution function with the Polyakov loop tends to decrease the HQ transport coefficient, the Debye mass has the effect of increasing these transport coefficients. We have found a weak temperature dependence of the heavy quark drag coefficient with a Polyakov loop value taken from PQM, which is consistent with other models like the $T$-matrix and quasiparticle models, which also take into account the nonperturbative effects in a different manner. This consistency suggests the existence of possible model-independent correlations between the results obtained with the Polyakov loop and other nonperturbative models and reaffirms the temperature and momentum dependence of heavy quark transport coefficients. In the present investigation, we have confined our attention to the elastic $2 \to 2$ processes within the matrix model. The inclusion of other effects arising from $2 \to 3$ processes and LPM effects are expected to be subdominant due to the large mass of the heavy quark [65], but nonetheless can be important at high parton density. We plan to explore different possible phenomenological implications of the present investigation in the future.

## ACKNOWLEDGMENTS

S. K. D. acknowledges support by the National Science Foundation of China (Grants No. 11805087 and No. 11875153). We would like to thank Yoshimasa Hidaka for valuable discussions and important clarifications on the HTL resummed propagator in the presence of a Polyakov loop.

## APPENDIX A: POLYAKOC LOOP EXTENDED QUARK-MESON MODEL

The Polyakov loop extended quark-meson model (PQM) captures two important features of quantum chromodynamics (QCD): namely, chiral symmetry breaking and its restoration at high temperature and density, as well as the confinement-deconfinement transitions. Explicitly, the Lagrangian of the PQM model is given by [37–41]

$$\mathcal{L} = \bar{\psi}(i\gamma^\mu D_\mu - m - g_\sigma(\sigma + i\gamma_5 \boldsymbol{\tau}\cdot\boldsymbol{\pi}))\psi + \frac{1}{2}[\partial_\mu\sigma\partial^\mu\sigma + \partial_\mu\boldsymbol{\pi}\partial^\mu\boldsymbol{\pi}] - U_\chi(\sigma,\boldsymbol{\pi}) - U_P(\phi,\bar{\phi}). \tag{A1}$$

In the above, the first term is the kinetic and interaction term for the quark doublet $\psi = (u, d)$ interacting with the scalar ($\sigma$) and the isovector pseudoscalar pion ($\boldsymbol{\pi}$) field. The scalar field $\sigma$ and the pion field $\boldsymbol{\pi}$ together form a $SU(2)$ isovector field. The quark field is also coupled to a spatially constant temporal gauge field $A_0$ through the covariant derivative $D_\mu = \partial_\mu - ieA_\mu$; $A_\mu = \delta_{\mu 0}A_\mu$.

The mesonic potential $U_\chi(\sigma,\pi)$ essentially describes the chiral symmetry-breaking pattern in the strong interaction and is given by

$$U_\chi(\sigma,\boldsymbol{\pi}) = \frac{\lambda}{4}(\sigma^2 + \boldsymbol{\pi}^2 - v^2) - c\sigma. \tag{A2}$$

The last term in the Lagrangian in Eq. (A1) is responsible for including the physics of color confinement in terms of a potential energy for the expectation values of the Polyakov loop $\phi$ and $\bar{\phi}$, which are defined in terms of the Polyakov loop operator, which is a Wilson loop in the temporal direction:

$$\mathcal{P} = P\exp\left(i\int_0^\beta dx_0 A_0(x_0,\mathbf{x})\right). \tag{A3}$$

In the Polyakov gauge, $A_0$ is time independent and is in the Cartan subalgebra; i.e., $A_0^a = A_0^3\lambda_3 + A_0^8\lambda_8$. One can perform the integration over the time variable trivially as path ordering becomes irrelevant, so that $\mathcal{P}(\mathbf{x}) = \exp(\beta A_0)$. The Polyakov loop variable $\phi$ and its Hermitian conjugate $\bar{\phi}$ are defined as

$$\phi(\mathbf{x}) = \frac{1}{N_c} Tr\mathcal{P}(\mathbf{x}), \qquad \bar{\phi}(\mathbf{x}) = \frac{1}{N_c}\mathcal{P}^{\dagger}(\mathbf{x}). \tag{A4}$$

In the limit of heavy quark mass, the confining phase is center symmetric, and therefore $\langle\phi\rangle = 0$, while for the deconfined phase $\langle\phi\rangle \neq 0$. Finite quark masses break this symmetry explicitly. The explicit form of the potential $U_p(\phi, \bar{\phi})$ is not known from first-principle calculations. The common strategy is to choose a functional form of the potential that reproduces the pure gauge lattice simulation thermodynamic results. Several forms of this potential have been suggested in literature. We shall use here the following polynomial parametrization [37]:

$$U_P(\phi, \bar{\phi}) = T^4\left[-\frac{b_2(T)}{2}\bar{\phi}\phi - \frac{b_3}{2}(\phi^3 + \bar{\phi}^3) + \frac{b_4}{4}(\bar{\phi}\phi)^2\right], \tag{A5}$$

with the temperature-dependent coefficient $b_2$ given as

$$b_2(T) = a_0 + a_1\left(\frac{T_0}{T}\right) + a_2\left(\frac{T_0}{T}\right)^2 + a_3\left(\frac{T_0}{T}\right)^3. \tag{A6}$$

The numerical values of the parameters are

$$a_0 = 6.75, \quad a_1 = -1.95, \quad a_2 = 2.625, \quad a_3 = -7.44, \tag{A7}$$

$$b_3 = 0.75, \qquad b_4 = 7.5. \tag{A8}$$

The parameter $T_0$ corresponds to the transition temperature of Yang-Mills theory. However, for the full dynamical QCD, there is a flavor dependence on $T_0(N_f)$. For two flavors, we take it to be $T_0(2) = 192$ MeV, as in Ref. [37].

The Lagrangian in Eq. (A1) is invariant under $SU(2)_L \times SU(2)_R$ transformation when the explicit symmetry-breaking term $c\sigma$ vanishes in the potential $U_\chi$ in Eq. (A2). The parameters of the potential $U_\chi$ are chosen such that the chiral symmetry is spontaneously broken in the vacuum. The expectation values of the meson fields in vacuum are $\langle\sigma\rangle = f_\pi$ and $\langle\boldsymbol{\pi}\rangle = 0$. Here $f_\pi = 93$ MeV is the pion decay constant. The coefficient of the symmetry-breaking linear term is decided from the partial conservation of the axial vector current (PCAC) as $c = f_\pi m_\pi^2$, $m_\pi = 138$ MeV, being the pion mass. Then, by minimizing the potential, one has $v^2 = f_\pi^2 - m_\pi^2/\lambda$. The quartic coupling for the meson, and $\lambda$ is determined from the mass of the sigma meson given as $m_\sigma^2 = m_\pi^2 + 2\lambda f_\pi^2$. In the present work, we take $m_\sigma = 600$ MeV, which gives $\lambda = 19.7$. The coupling $g_\sigma$ is fixed here from the constituent quark mass in vacuum, $M_q = g_q f_\pi$, which has to be about one third of the nucleon mass that leads to $g_\sigma = 3.3$ [66].

To calculate the bulk thermodynamical properties of the system, we use a mean field approximation for the meson and the Polyakov fields while retaining the quantum and thermal fluctuations of the quark fields. The thermodynamic potential can then be written as

$$\Omega(T, \mu) = \Omega_{\bar{q}q} + U_\chi + U_P(\phi, \bar{\phi}). \tag{A9}$$

The fermionic part of the thermodynamic potential is given as

$$\Omega_{\bar{q}q} = -2N_f T\int\frac{d^3p}{(2\pi)^3}[\ln(1 + 3(\phi + \bar{\phi}e^{-\beta\omega_-})e^{-\beta\omega_-} + e^{-3\beta\omega_-}) + \ln(1 + 3(\phi + \bar{\phi}e^{-\beta\omega_+})e^{-\beta\omega_+} + e^{-3\beta\omega_+})] \tag{A10}$$

modulo a divergent vacuum part. In the above, $\omega_\mp = E_p \mp \mu$, with the single-particle quark-antiquark energy $E_p = \sqrt{\mathbf{p}^2 + M^2}$. The constituent quark-antiquark mass is defined to be

$$M^2 = g_\sigma^2(\sigma^2 + \pi^2). \tag{A11}$$

The divergent vacuum part arises from the negative-energy states of the Dirac sea. Using standard renormalization, it can be partly absorbed in the coupling $\lambda$ and $v^2$. However, a logarithmic correction from the renormalization scale remains, which we neglect in the calculations that follow [66].

The mean fields are obtained by minimizing $\Omega$ with respect to $\sigma$, $\phi$, $\bar{\phi}$, and $\pi$. Extremizing the effective potential with respect to the $\sigma$ field leads to

$$\lambda(\sigma^2 + \pi^2 - v^2) - c + g_\sigma\rho_s = 0, \tag{A12}$$

where the scalar density $\rho_s = -\langle\bar{\psi}\psi\rangle$ is given by

$$\rho_s = 6N_f g_\sigma\sigma\int\frac{d\mathbf{p}}{(2\pi)^3}\frac{1}{E_P}[f_-(\mathbf{p}) + f_+(\mathbf{p})]. \tag{A13}$$

In the above, $f_\mp(\mathbf{p})$ are the distribution functions for the quarks and antiquarks, given as

$$f_-(\mathbf{p}) = \frac{\phi e^{-\beta\omega_-} + 2\bar{\phi}e^{-2\beta\omega_-} + e^{-3\beta\omega_-}}{1 + 3\phi e^{-\beta\omega_-} + 3\bar{\phi}e^{-2\beta\omega_-} + e^{-3\beta\omega_-}} \tag{A14}$$

and

$$f_+(\mathbf{p}) = \frac{\bar{\phi}e^{-\beta\omega_+} + 2\phi e^{-2\beta\omega_+} + e^{-3\beta\omega_+}}{1 + 3\bar{\phi}e^{-\beta\omega_+} + 3\phi e^{-2\beta\omega_+} + e^{-3\beta\omega_+}}. \tag{A15}$$

The condition $\frac{\partial\Omega}{\partial\phi} = 0$ leads to

$$T^4\left[-\frac{b_2}{2}\bar{\phi} - \frac{b_3}{2}\phi^2 + \frac{b_4}{2}\bar{\phi}\phi\bar{\phi}\right] + I_\phi = 0, \tag{A16}$$

where

$$I_\phi = \frac{\partial\Omega_{\bar{q}q}}{\partial\phi} = -6N_f T\int\frac{d\mathbf{p}}{(2\pi)^3}\left[\frac{e^{-\beta\omega_-}}{1+3\phi e^{-\beta\omega_-}+3\bar{\phi}e^{-2\beta\omega_-}+e^{-3\beta\omega_-}} + \frac{e^{-2\beta\omega_+}}{1+3\bar{\phi}e^{-\beta\omega_+}+3\phi e^{-2\beta\omega_+}+e^{-3\beta\omega_+}}\right]. \tag{A17}$$

Similarly, $\frac{\partial\Omega}{\partial\bar{\phi}} = 0$ leads to

$$T^4\left[-\frac{b_2}{2}\phi - \frac{b_3}{2}\bar{\phi}^2 + \frac{b_4}{2}\bar{\phi}\phi^2\right] + I_{\bar{\phi}} = 0, \tag{A18}$$

with

$$I_{\bar{\phi}} = \frac{\partial\Omega_{\bar{q}q}}{\partial\bar{\phi}} = -6N_f T\int\frac{d\mathbf{p}}{(2\pi)^3}\left[\frac{e^{-2\beta\omega_-}}{1+3\phi e^{-\beta\omega_-}+3\bar{\phi}e^{-2\beta\omega_-}+e^{-3\beta\omega_-}} + \frac{e^{-\beta\omega_+}}{1+3\phi e^{-\beta\omega_+}+3\bar{\phi}e^{-2\beta\omega_+}+e^{-3\beta\omega_+}}\right]. \tag{A19}$$

By solving Eqs. (A12), (A16), and (A18) self-consistently, one can get the values of the constituent quark mass, the Polyakov loop variable, and the conjugate Polyakov loop variable as a function of temperature.

## APPENDIX B: SCATTERING AMPLITUDES

There are two types of scattering that contribute to the drag and the diffusion coefficients: namely, Coulomb scattering i.e., scattering off of HQs from light quarks—and Compton scattering i.e., scattering off of gluons from HQs [45]. The dominant contribution for these scatterings arise from the gluon exchange in the $t$ channel, which is infrared divergent [16,47]. This is regularized by introducing the Debye screening [16,45], which we have evaluated in the HTL limit in the background of a Polyakov loop. In the $s$ and $u$ channels, however, there is no such infrared divergence. Note that the matrix model, $m_D$, in Eq. (60), is color dependent, so the propagator is also color dependent. For $N_f$ flavor of light quark, the spin-averaged matrix element squared for Coulomb scattering, as shown on the left side of Fig. 10, can be written as

$$|\mathcal{M}_C|^2 = \frac{16N_f g^4}{8N}\mathcal{P}^{cd}_{ae}\mathcal{P}^{ml}_{bf}\mathcal{P}^{c'd'}_{ea}\mathcal{P}^{m'l'}_{fb}\frac{((s-m^2-M^2)^2+(u-m^2-M^2)^2+2(M^2+m^2)t)}{(t+(m_D^2)_{mlcd})(t+(m_D^2)_{m'l'c'd'})}. \tag{B1}$$

where $a$, $b$ ($e$, $f$) are color indices of initial (light, heavy) and final (light, heavy) quarks. For calculational simplifications, one can take the color-averaged Debye mass as defined in Eq. (61) so that $(m_D^2)_{mlcd} \approx \bar{m}_D^2\mathcal{P}_{mlcd}$. In this case, we get

$$\mathcal{P}^{cd}_{ae}\mathcal{P}^{ml}_{bf}\frac{1}{(t+(m_D^2)_{mlcd})} = \frac{1}{t+\bar{m}_D^2\mathcal{P}^{fb}_{ae}} - \frac{1}{N}\left(\frac{2}{t+\bar{m}_D^2} - \frac{1}{N}\frac{1}{t+\bar{m}_D^2}\right)\delta_{ae}\delta_{fb}. \tag{B2}$$

One can further simplify the expression in Eq. (B1) by taking the leading-order contribution in $N$. With this assumption, Eq. (B1) reduces to

$$|\mathcal{M}_C|^2_{abef} = \frac{8g^4}{2N}\delta^f_a\delta^b_e\frac{((s-m^2-M^2)^2+(u-m^2-M^2)^2+2(M^2+m^2)t)}{(t+(\bar{m}_D^2)^2)^2}, \tag{B3}$$

where $M$ is the HQ mass. For the $q^aQ^b \to q^eQ^f$ scattering, the product of the distribution function and matrix element squared that appears in Eq. (15) can be simplified by summing over colors of the initial and final light/heavy quarks. Note that for light quarks, the colors appearing in Eq. (B3) have to be summed with the distribution function and can be written as

$$\delta^f_a\delta^b_e f(q)_e(1-f(q')_f) = N^2 f(q)_q(1-f(q')_q), \tag{B4}$$

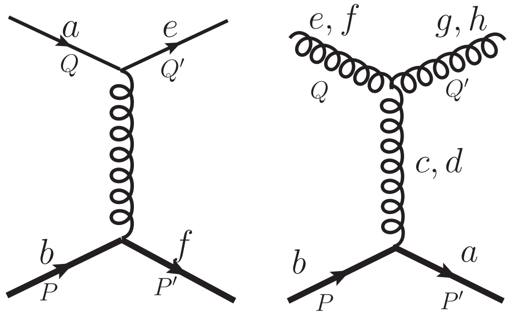


FIG. 10. Coulomb scattering (left) of HQs (bold solid line) and light quarks/antiquarks (thin solid line). $t$-channel Compton scattering (right).

where $f(q)_q$ is the average distribution function of the quark as defined in Eq. (22). Similarly, for the $t$-channel Compton scattering shown on the right side of Fig. 10, one can write

$$|\mathcal{M}_t|^2 = \frac{g^4}{4(N^2-1)} \mathcal{P}^{ml}_{ba} \mathcal{P}^{l'm'}_{ab} f^{cd,ef,gh} f^{d'c',fe,hg} \times \left( \frac{16(s-M^2)(M^2-u)}{(t+(m_D^2)_{mlcd})(t+(m_D^2)_{m'l'c'd'})} \right) \tag{B5}$$

and can be simplified in a similar way as done for Coulomb scattering. Here $ef, b$ $(gh, a)$ are the color indices for the initial (final) gluon and quark. The scattering amplitude of $u$-channel Compton scattering shown on the right side of Eq. (11) can be written as

$$|\mathcal{M}_u|^2 = \frac{8g^4}{8(N^2-1)} \mathcal{P}^{gh}_{bc} \mathcal{P}^{gh}_{bc'} \mathcal{P}^{ef}_{ca} \mathcal{P}^{ef}_{c'a} \times \left( \frac{M^4 - us + M^2(3u+s)}{(u-M^2)^2} \right). \tag{B6}$$

Note here that the propagator has no color-dependent term. The matrix element squared for $s$-channel Compton scattering, as shown on the left side of Fig. 11, is

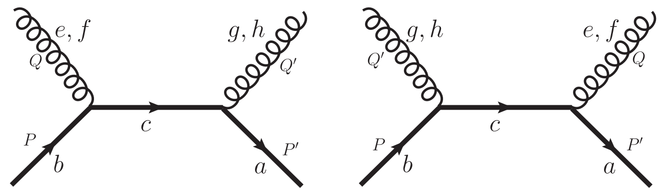


FIG. 11. $s$-channel Compton scattering (left). $u$-channel Compton scattering (right).

$$|\mathcal{M}_s|^2 = \frac{8g^4}{8(N^2-1)} \mathcal{P}^{ef}_{bc} \mathcal{P}^{ef}_{bc'} \mathcal{P}^{gh}_{ca} \mathcal{P}^{gh}_{c'a} \times \left( \frac{M^4 - us + M^2(u+3s)}{(s-M^2)^2} \right). \tag{B7}$$

There are interferences between different scatterings contributing to $g^{ef} Q^b \to g^{gh} Q^a$ that can be written as

$$\mathcal{M}_s \mathcal{M}_u{}^\dagger = \mathcal{M}_u \mathcal{M}_s{}^\dagger = \frac{g^4}{8(N^2-1)} \mathcal{P}^{ef}_{bc} \mathcal{P}^{gh}_{ca} \mathcal{P}^{gh}_{bc'} \mathcal{P}^{ef}_{c'a} \times \left( \frac{32M^4 - 8M^2 t}{(s-M^2)(u-M^2)} \right), \tag{B8}$$

$$\mathcal{M}_s \mathcal{M}_t{}^\dagger = \mathcal{M}_s^\dagger \mathcal{M}_t = \frac{g^4}{4\sqrt{2}(N^2-1)} \mathcal{P}^{ef}_{bc} \mathcal{P}^{gh}_{ca} \mathcal{P}^{lm}_{ab} (i f^{dc,fe,hg}) \times \left( \frac{-8(M^4 - 2M^2 s + us)}{(s-M^2)(t+(m_D^2)_{mlcd})} \right), \tag{B9}$$

$$\mathcal{M}_u \mathcal{M}_t{}^\dagger = \mathcal{M}_u^\dagger \mathcal{M}_t = \frac{g^4}{4\sqrt{2}(N^2-1)} \mathcal{P}^{gh}_{bc} \mathcal{P}^{ef}_{ca} \mathcal{P}^{lm}_{ab} (i f^{dc,fe,hg}) \times \left( \frac{8(4M^4 - M^2 t)}{(u-M^2)((t+(m_D^2)_{mlcd}))} \right). \tag{B10}$$

The total matrix element squared that contributes to Compton scattering (i.e., $gQ \to gQ$) is $|\mathcal{M}_{Cm}|^2_{abefgh} = |\mathcal{M}_s|^2 + |\mathcal{M}_u|^2 + |\mathcal{M}_t|^2 + \mathcal{M}_u \mathcal{M}_s^\dagger + \mathcal{M}_s \mathcal{M}_u^\dagger + \mathcal{M}_t \mathcal{M}_s^\dagger + \mathcal{M}_s \mathcal{M}_t^\dagger + \mathcal{M}_u \mathcal{M}_t^\dagger + \mathcal{M}_t \mathcal{M}_u^\dagger$. These matrix elements are used in Eq. (15) to estimate the drag and the diffusion coefficient.

[1] E. V. Shuryak, Nucl. Phys. A750, 64 (2005).
[2] B. V. Jacak and B. Muller, Science 337, 310 (2012).
[3] F. Prino and R. Rapp, J. Phys. G 43, 093002 (2016).
[4] A. Andronic et al., Eur. Phys. J. C 76, 107 (2016).
[5] V. Greco, Nucl. Phys. A967, 200 (2017).
[6] G. Aarts et al., Eur. Phys. J. A 53, 93 (2017).
[7] R. Rapp et al., Nucl. Phys. A979, 21 (2018).
[8] S. Cao et al., Phys. Rev. C 99, 054907 (2019).
[9] X. Dong and V. Greco, Prog. Part. Nucl. Phys. 104, 97 (2019).
[10] M. Cacciari, P. Nason, and R. Vogt, Phys. Rev. Lett. 95, 122001 (2005).
[11] M. Djordjevic, M. Gyulassy, R. Vogt, and S. Wicks, Phys. Lett. B 632, 81 (2006).
[12] N. Armesto, M. Cacciari, A. Dainese, C. A. Salgado, and U. A. Wiedemann, Phys. Lett. B 637, 362 (2006).
[13] B. I. Abelev et al. (STAR Collaboration), Phys. Rev. Lett. 98, 192301 (2007).
[14] A. Adare et al. (PHENIX Collaboration), Phys. Rev. Lett. 98, 172301 (2007).

[15] S. S. Adler *et al.* (PHENIX Collaboration), Phys. Rev. Lett. **96**, 032301 (2006).

[16] G. D. Moore and D. Teaney, Phys. Rev. C **71**, 064904 (2005).

[17] H. van Hees, V. Greco, and R. Rapp, Phys. Rev. C **73**, 034913 (2006).

[18] H. van Hees, M. Mannarelli, V. Greco, and R. Rapp, Phys. Rev. Lett. **100**, 192301 (2008).

[19] M. He, R. J. Fries, and R. Rapp, Phys. Rev. C **86**, 014903 (2012).

[20] S. K. Das, F. Scardina, S. Plumari, and V. Greco, Phys. Lett. B **747**, 260 (2015).

[21] F. Scardina, S. K. Das, V. Minissale, S. Plumari, and V. Greco, Phys. Rev. C **96**, 044905 (2017).

[22] S. K. Das, V. Chandra, and J. e. Alam, J. Phys. G **41**, 015102 (2014).

[23] H. Berrehrah, E. Bratkovskaya, W. Cassing, P. B. Gossiaux, J. Aichelin, and M. Bleicher, Phys. Rev. C **89**, 054901 (2014).

[24] T. Song, H. Berrehrah, D. Cabrera, J. M. Torres-Rincon, L. Tolos, W. Cassing, and E. Bratkovskaya, Phys. Rev. C **92**, 014910 (2015).

[25] P. B. Gossiaux and J. Aichelin, Phys. Rev. C **78**, 014904 (2008).

[26] W. M. Alberico, A. Beraudo, A. De Pace, A. Molinari, M. Monteno, M. Nardi, and F. Prino, Eur. Phys. J. C **71**, 1666 (2011).

[27] T. Lang, H. van Hees, J. Steinheimer, G. Inghirami, and M. Bleicher, Phys. Rev. C **93**, 014901 (2016).

[28] Y. Xu, J. E. Bernhard, S. A. Bass, M. Nahrgang, and S. Cao, Phys. Rev. C **97**, 014907 (2018).

[29] S. Cao, T. Luo, G. Y. Qin, and X. N. Wang, Phys. Rev. C **94**, 014909 (2016).

[30] C. A. G. Prado, J. Noronha-Hostler, R. Katz, A. A. P. Suaide, J. Noronha, M. G. Munhoz, and M. R. Cosentino, Phys. Rev. C **96**, 064903 (2017).

[31] M. Nahrgang, J. Aichelin, S. Bass, P. B. Gossiaux, and K. Werner, Phys. Rev. C **91**, 014904 (2015).

[32] S. Plumari, V. Minissale, S. K. Das, G. Coci, and V. Greco, Eur. Phys. J. C **78**, 348 (2018).

[33] S. K. Das, M. Ruggieri, S. Mazumder, V. Greco, and J. e. Alam, J. Phys. G **42**, 095108 (2015).

[34] K. Fukushima, Phys. Rev. D **77**, 114028 (2008).

[35] C. Ratti, S. Roessner, M. A. Thaler, and W. Weise, Eur. Phys. J. C **49**, 213 (2007).

[36] P. Costa, C. A. de Sousa, M. C. Ruivo, and H. Hansen, Europhys. Lett. **86**, 31001 (2009).

[37] B. J. Schaefer, J. M. Pawlowski, and J. Wambach, Phys. Rev. D **76**, 074023 (2007).

[38] U. S. Gupta and V. K. Tiwari, Phys. Rev. D **85**, 014010 (2012).

[39] B. W. Mintz, R. Stiele, R. O. Ramos, and J. S. Bielich, Phys. Rev. D **87**, 036004 (2013).

[40] S. Carignano, M. Buballa, and W. Elkamhawy, Phys. Rev. D **94**, 034023 (2016).

[41] H. Mishra and R. K. Mohapatra, Phys. Rev. D **95**, 094014 (2017).

[42] A. Abhishek, H. Mishra, and S. Ghosh, Phys. Rev. D **97**, 014005 (2018).

[43] Y. Hidaka, S. Lin, R. D. Pisarski, and D. Satow, J. High Energy Phys. 10 (2015) 005.

[44] S. Lin, R. D. Pisarski, and V. V. Skokov, Phys. Lett. B **730**, 236 (2014).

[45] B. Svetitsky, Phys. Rev. D **37**, 2484 (1988).

[46] Y. Hidaka and R. D. Pisarski, Phys. Rev. D **80**, 036004 (2009).

[47] R. Rapp and H. van Hees, arXiv:0903.1096.

[48] E. M. Lifshitz and L. P. Pitaevskii, *Physical Kinetics* (Butterworth-Hienemann, Oxford, 1981).

[49] M. Golam Mustafa, D. Pal, and D. Kumar Srivastava, Phys. Rev. C **57**, 889 (1998); **57**, 3499(E) (1998).

[50] S. K. Das, J. E. Alam, and P. Mohanty, Phys. Rev. C **80**, 054916 (2009).

[51] H. van Hees and R. Rapp, Phys. Rev. C **71**, 034907 (2005).

[52] S. Plumari, W. M. Alberico, V. Greco, and C. Ratti, Phys. Rev. D **84**, 094004 (2011).

[53] Y. Hidaka and R. D. Pisarski, Phys. Rev. D **81**, 076002 (2010).

[54] A. Dumitru, Y. Guo, Y. Hidaka, C. P. K. Altes, and R. D. Pisarski, Phys. Rev. D **83**, 034022 (2011).

[55] G. 't Hooft, Nucl. Phys. **B72**, 461 (1974).

[56] P. Cvitanovic, Phys. Rev. D **14**, 1536 (1976).

[57] M. L. Bellac, *Thermal Field Theory* (Cambridge University Press, Cambridge, 1996).

[58] M. H. Thoma, arXiv:hep-ph/0010164.

[59] A. Bazavov, N. Brambilla, H.-T. Ding, P. Petreczky, H.-P. Schadler, A. Vairo, and J. H. Weber, Phys. Rev. D **93**, 114502 (2016).

[60] B. L. Combridge, Nucl. Phys. **B151**, 429 (1979).

[61] W. E. Caswell, Phys. Rev. Lett. **33**, 244 (1974).

[62] S. Y. F. Liu and R. Rapp, arXiv:1612.09138.

[63] S. Y. F. Liu and R. Rapp, Phys. Rev. C **97**, 034918 (2018).

[64] S. Y. F. Liu, M. He, and R. Rapp, Phys. Rev. C **99**, 055201 (2019).

[65] B. W. Zhang, E. Wang, and X. N. Wang, Phys. Rev. Lett. **93**, 072301 (2004).

[66] O. Scavenius, A. Mocsy, I. N. Mishustin, and D. H. Rischke, Phys. Rev. C **64**, 045202 (2001).